Bulletin of the Geological Survey of Japan, vol.52 (10), p.471-491, 2001

Genesis of Late Cretaceous-Paleogene Granitoids with Contrasting Chemical Trends in the Chubu District, Central Japan

Shunso ISHIHARA[1] and Chengyu WU[2]

Shunso ISHIHARA and Chengyu WU (2001) Genesis of late Cretaceous-Paleogene granitoids with contrasting chemical trends in the Chubu District, central Japan. *Bull. Geol. Surv. Japan*, vol. 52 (10), p.471-491, 9 figs., 1 table, 3 appendices.

Abstract: Late Cretaceous to Paleogene rhyolites (11 samples) and granitoids (Shirakawa 29, Toki 7, Naegi 9, Ryoke 10; total 55 samples), which have high intial Sr ratios, were analyzed by XRF and ICP-MS for 11 major elements and 32 trace elements. Granitoids of the Shirakawa area intruding the Nohi Rhyolites in the Hida metamorphic terrane, belong to I-type magnetite series and contain commonly mafic enclaves. They are composed of a high Na_2O group of monzodiorite to granodiorite and a low-Na_2O group of biotite granites. The former is rich in mafic and calcic components, and was generated in mafic igneous source rocks of the Hida metamorphic terrane. The latter is felsic and leucogranitic, yet its Rb/Sr is not high enough to be a fractionated magma. The leucogranite, typically of the Hirase body, could be a minimum melt generated from an intermediate igneous source. The Shirakawa granitoids are depleted in Y and HREE, implying the existence of garnet and hornblende in the source region.

Late Cretaceous-Paleogene granitoids occurring in the Mino sedimentary terrane belong to I-type ilmenite-series composed of high-level plutons of the Toki and Naegi areas and intermediate-level plutons of the Ryoke granitoids. These granitoids are reduced and per-aluminous implying genetic connection with sedimentary and less igenous sources. The Toki and Naegi bodies are composed mostly of biotite granite, intruding discordantly, and are rich in lithophile elements. The Naegi granite is especially high in Rb, Y, Th, and U and its Rb/Sr ratio is the highest among the studied rocks. Its REE pattern is flat with high HREE and a strong Eu anomaly, which could be considered as fractionated I type. The Ryoke granitoids are mostly biotite granite but horblende-biotite granodiorite is also common. They are less fractionated and have own geochemical characters compared with the Toki and Naegi granites. The studied granitoids have chemical compositions reflecting basically their basement characteristics, and also partly their degree of the magmatic fractionation.

1. Introduction

Parallelism between magnetite-series and ilmenite-series granitic belts is widely known along the Japanese Island arcs in late Cretaceous and Miocene granitic and volcanic belts (Ishihara, 1971b, 1973). In the Inner Zone batholith of Southwest Japan (Ishihara, 1990), magnetite-series granitoids tend to occur along the back-arc side of the Sanin-Shirakawa belt, while ilmenite-series granitoids are distributed in the fore-arc side of the Sanyo and Ryoke belts. This parallelism was considered to reflect the chemical contrast of the source region for the granitic magmas (Ishihara and Terashima, 1977a).

In the Chubu District (Fig. 1), one of the type areas for magnetite- and ilmenite-series granitoids across the Honshu Island, the most distinctive feature is that, although Shirakawa granitoids of the Sanin-Shirakawa Belt to the north being mainly magnetite-bearing and granitoids of the Sanyo and Ryoke Belts to the south being generally magnetite-free ilmenite-series; both the magnetite- and ilmenite-series granitoids have the same latest Cretaceous-Paleogene age and similar high $^{87}Sr/^{86}Sr$ initial ratios ranging from 0.7096 to 0.7106 (Shibata and Ishihara, 1979a, b). The district is char-

[1] Institute of Geoscience, GSJ. s-ishihara@aist.go.jp
[2] Rio Tinto Mining & Exploration Ltd., 1821, Tower 2, China World Trade Centre, 1 Jianguomenwei Ave., Beijing 100004, China

Keywords: Late Cretaceous-Paleogene, granitoids, major chemistry, trace elements, Nohi Rhyolites, Shirakawa granitoids, Naegi Granite

acterized by gravity low in the northern part of the Hida metamorphic terrane (Komazawa *et al.*, 1999), reflecting a thick continental crust. These granitoids of this district having I-type characteristics (Chappell and White, 1992), should have originated within or greatly influenced by the continental crust.

Regional chemical variations of the granitoids across the Shirakawa-Toki-Okazaki transect were s lied by Ishihara and Terashima (1977a), who showed high Fe_2O_3/FeO ratios in the Shirakawa area and low Fe_2O_3/FeO ratios in the Sanyo-Ryoke Belts. The oxidized magmas were considered to reflect the high Fe_2O_3/FeO ratio of the source rocks, while the reduced magmas were interpreted to have been reduced by organic carbon from the accretionary sedimentary complex (Ishihara, 1984). In addition, a "constant-type" and an "increasing-type" for some lithophile elements plotted against the differentiation index, such as F, Li, Rb, Pb, Sn and Be in highly fractionated granites, were observed on the Shirakawa granitoids and the Toki-Naegi granites, respectively. These granitoids are also different in associated mineralizations: economic amounts of molybdenum deposits in the Shirakawa area, but tin-bearing tungsten deposits in the Naegi area (Ishihara, 1973). REE- and U-Th-bearing minerals are nearly absent in the Shirakawa area, except for xenotime discovered in pegmatitic quartz vein of the Hirase deposit (Ishihara, 1971a), but are very abundant in small but many pegmatites within the Naegi granite.

In order to understand the genesis of these two constrasting granitoid series, and also to detail the genetic variations within the Shirakawa and Naegi-Toki areas, a detailed chemical study was made here for major and trace elements on 66 samples, including 29 from Shirakawa granitoids, 26 from Toki, Naegi and Ryoke I granites and 11 from sorrounding rhyolitic country rocks. The analytical methods are XRF with glass-bead for major elements and pressed powder pellets for minor elements (V, Ni, Ga, Rb, Sr, Ba, Y, Zr, Th and U), ICP-MS with acid digestion (Li, Be, Sc, Cu, Zn, Rb, Sr, Ba, Ga and Mo), and fusion decomposition (Y, Zr, Nb, Sn, Cs, Hf, Ta Pb, Th and U). Details are given in Wu *et al.* (1993) and Wu and Ishihara (1994). The analytical results are listed in Appendices 1 through 3 and the studied areas are shown in Figs. 1 through 3.

2. Geologic Background

2.1 Shirakawa Area

The Shirakawa granitoids located in the Hida metamorphic terrane of Hida gneisses and Triassic-Jurassic I-type Funatsu granitoids, occur as a group of granitic stocks intruding coeval felsic welded tuffs called "Nohi Rhyolites", which have been classified into six sequences in the central and southern parts. Their

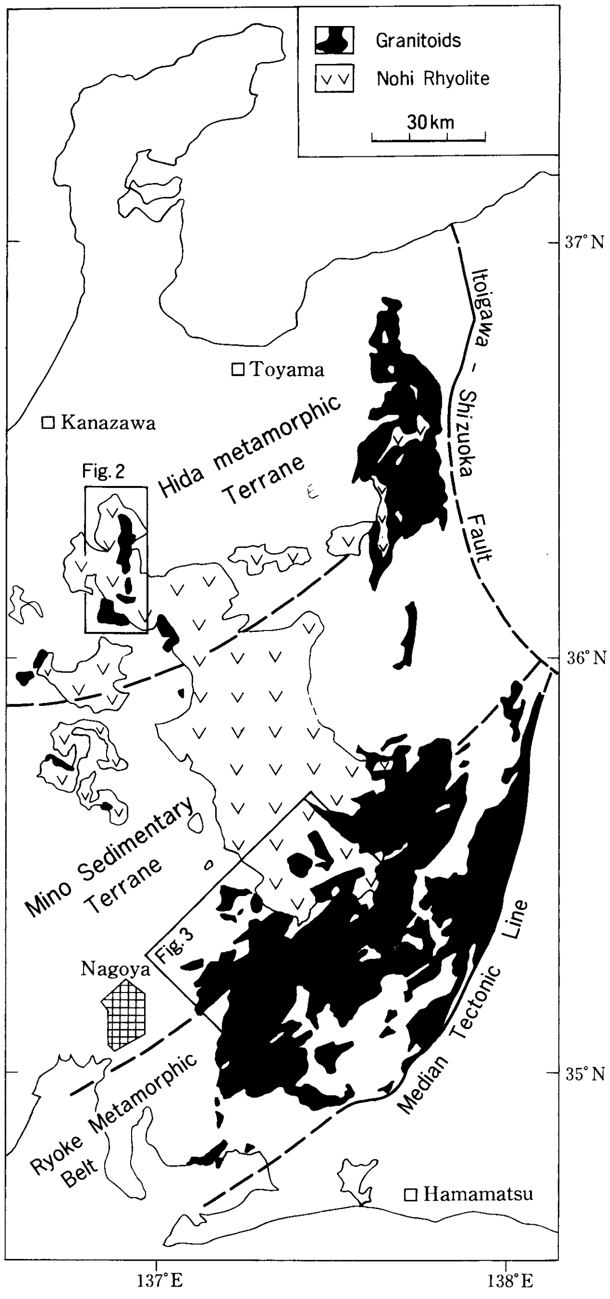

Fig. 1 Distribution of the late Cretaceous-Paleogene granitoids and associated Nohi rhyolites, and the studied areas in the Chubu District.

CHIME (Chemical Th-U-total Pb isochron method) and Rb-Sr ages vary from 86 to 56 Ma (Koido and Yamada, 1999). The main granitic bodies are, from north to south, Hatogaya (granodiorite to monzogranite, but referred here as granite), Hirase (granite), Mihoro (granodiorite), Awaradani (granodiorite) and Fukushimadani (granite) (Fig. 2). A Rb-Sr whole-rock isochron for these granitoids indicates an age of 65.6 ± 1.8Ma with the initial $^{87}Sr/^{86}Sr$ ratio of 0.7100 ± 0.0002 (Shibata and Ishihara, 1979a, b).

The granitoids comprise amphibole-biotite granodiorite and biotite granite. They are fine-grained and

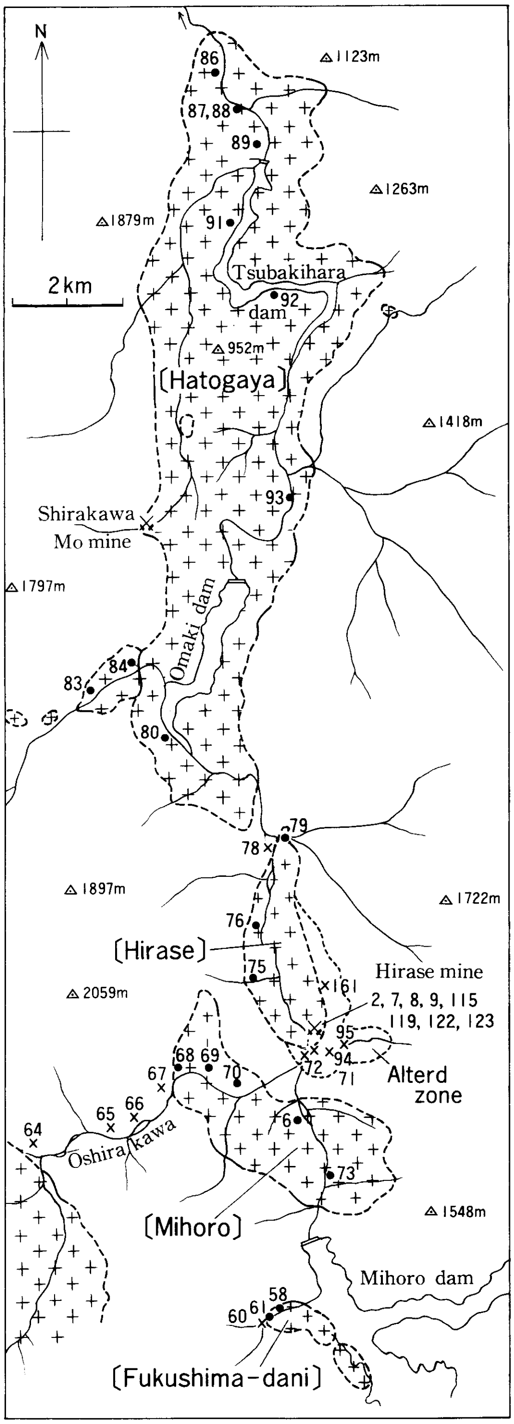

Fig. 2 Distribution of the Shirakawa granitoids (crossed part) and Nohi Rhyolites (blank part), and locality of the analyzed samples. ● granitoids; × Nohi Rhyolites, with the last two digits of the sample numbers in Appendices 1 and 2.

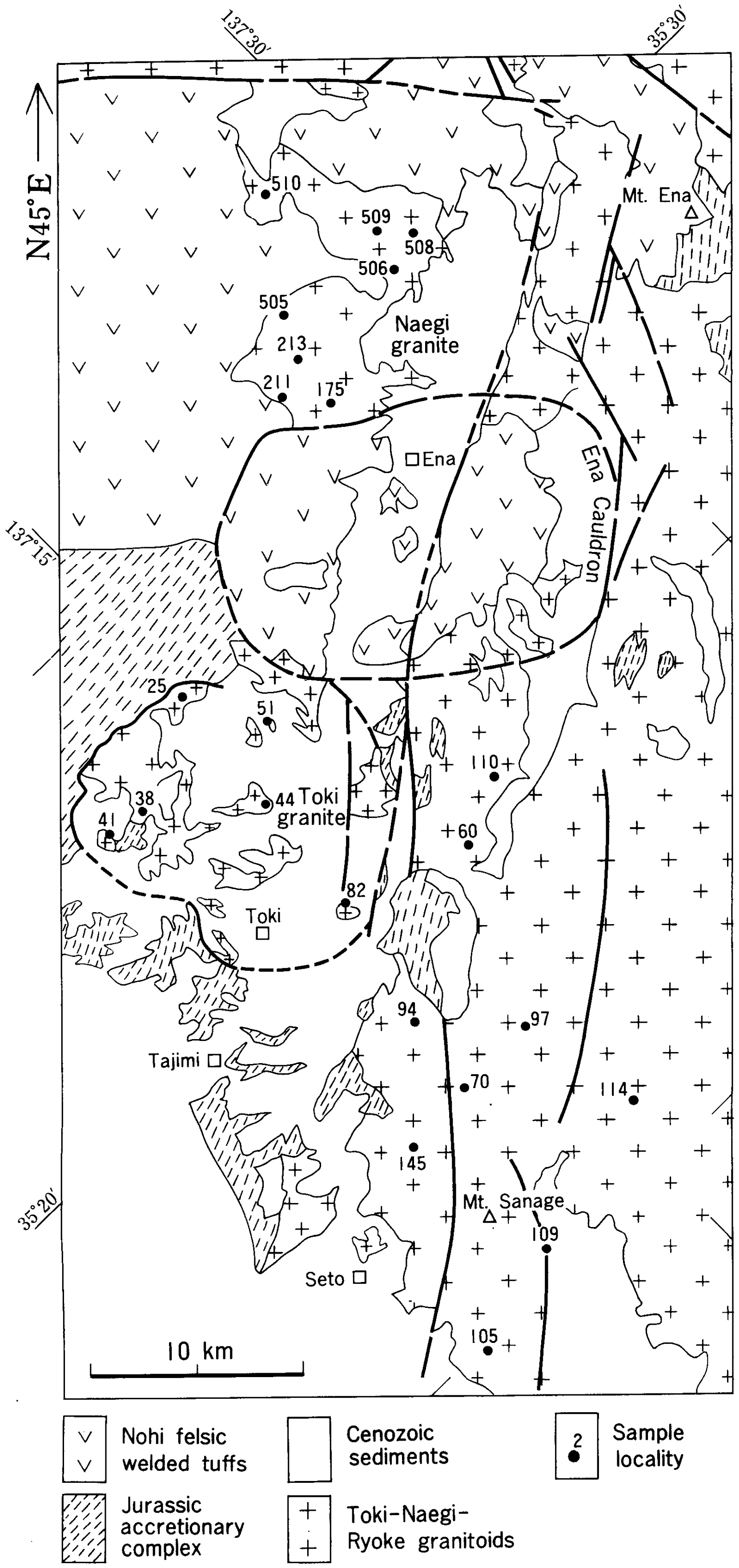

Fig. 3 Distribution of the Naegi-Toki-Ryoke granitoids, Chubu District. The Ena cauldron is taken from Yamada (1989). Solid circle, locality of the analyzed granitoids with the last two digits of the sample numbers in Appendix 3.

high level. The analyzed samples were selected from various bodies shown in Fig. 2. No sedimentary enclaves are present in the granitoids but mafic igneous enclaves are found. Conglomerate-looking mafic enclaves hosted in leucogranites (see Plate LXI of Ishihara, 1971a) are typically seen in the northern part of the Hatogaya body. The most mafic rock among the analyzed samples (Fig. 2), e.g., no. 88 (hereafter the last two digits on the sample numbers are shown), is such an enclave monzodiorite.

The Hirase body is composed of the main phase granite of $_{72}bG_3$, which should be read a biotite monzogranite with color index of 3 vol. percent (mostly biotite) and the grain-size index (number of grain boundary of the rock-forming minerals in 25 mm distance, see Ishihara, 1971a) of 72 and marginal finer phase of $_{142}b/mG_2$, which is finer, leucocratic phase with biotite and little muscovite. They can be called haplogranite of Tuttle and Bowen (1958).

The granitoids have A/CNK ratios (mol. $Al_2O_3/CaO + Na_2O + K_2O$) between 0.95 and 1.06 (Appendix 2), which are lower than the S-type limit of 1.1 (Chappell and White, 1992), implying all the granitoids belong to I type. The magnetic susceptibility varies from 765 x 10^{-6} for quartz monzodiorite to 100 x10^{-6} emu/g for granite. These are slightly lower than the typical values found in the major Mo-mineralized area of the Sanin district (Ishihara, 1971a). The Awaradani granodiorite body is an exception having the magnetic susceptibility lower than 100 x10^{-6} emu/g, being thus I-type/ilmenite series.

The Nohi Rhyolites, comprising mostly dacitic-rhyolitic pyroclastic rocks which have been welded, are considered to be comagmatic with the granitoids (Yamada, 1977). In the Shirakawa area, the Nohi Rhyolites have received a weak propylitic alteration and thermally metamorphosed by intrusion of the nearby granitoids; e.g., Fukushima-dani granite (see Plate LXI, Ishihara 1971a), and hydrothermally altered around the Mo-mineralized stock at Hirase. Thus, the alteration is considered to be "contact" hydrothermal alteration (Ishihara, 1971a), and shows following zones, from the Hirase granite outwards: (1) andalusite-biotite-sericite zone and/or (2) siderite-sericite zone, and then (3) calcite-chlorite zone.

Molybdenite-quartz veins are widely distributed in the Shirakawa area (Fig. 1). At the Hirase mine (Onishi *et al.*, 1973), hosted in leucogranite of the Hirase stock, production (1941-1974) of molybdenite concentrates amounts to 2,692 tons (MoS_2 97%). The next largest production of ca.40 tons comes from the Shirakawa Suien (Mo) veins occurring at the western margin of the Hatogaya stock. The Hirase veins striking N-S and dipping vertically contain beautiful euhedral crystals of molybdenite and accessory amounts of K-feldspar, xenotime, and base metal and iron sulfides. The vein walls have been carbonitized and sericitized, but not greisenized.

2.2 Naegi-Toki-Sanage Area

Around the southern margin of the Nohi Rhyolites, high-level granitoids intrude into the volcanic and subvolcanic rocks of the Nohi Rhyolites and Jurassic sedimentary rocks of the Mino accretionary complex (Fig. 1). The volcanic rocks are not exposed to the south but the sedimentary rocks which have been regionally metamorphosed, implying deeper levels of the granitoids, are seen in the southern area. All the granitoids have magnetic susceptibility below 12 - 18 x 10^{-6} emu/g, thus belonging to the ilmenite series.

2.2.1 Naegi Granite

The Naegi granite intrudes the southeastern margin of the Nohi Rhyolites (Fig. 3). The intrusion is controlled by NNW-trending faults, which correspond to the most distinct fracture system for the Nohi Rhyolites, and NE-trending faults which bound the Ryoke granitoids to the south. A cauldron structure, NW-SE 15 km by NE-SW 13 km, was proposed to the southwest of the Naegi granite (Yamada, 1989). The Naegi granite is magnetite-free biotite granite with a medium-grain size. It also includes very fine-grained chilled margin, called "Nukame" stone by building stone miners, which occurs along the western rim (Kawata, 1961). Four samples each were selected from the western part (nos. 175, 211, 213, 505) and the eastern part (nos. 506, 508, 509, 510). They show A/CNK ratio of 1.02 - 1.05 (Appendix 3).

The granite contains many drusy-type pegmatites, ranging from a few centimeters to a few tens of centimeters in diameter. The drusy pegmatites in particular are well known to contain beautiful crystals of smoky quartz, K-feldspar, micas and accessory amounts of zircon and its REE-rich variety of naegite, fergusonite, samarskite, monazite, allanite, enalite - a REE-rich variety of uranothorite, xenotime and gadolinite. According to Koseki and Matsubara (1961), these minerals were found in the following numbers of localities: naegite, (15 localities), fergusonite (11), monazite (6), samarskite (6), allanite (5), enalite (4), gadolinite (4), xenotime (4) and zircon (3). Wolframite-quartz vein deposits with greisenization are known to occur within granite (Fukuoka mine) and in pyroclastic rocks of the Nohi Rhyolites (Ebisu and Togane mines). Including minor ore deposits, the following metallogenic zonings are observed from the Naegi granite northward: I pegmatite zone, II W-Sn-Bi zone, III W-As-Bi zone, and IV Cu-Pb-Zn-As zone (Sakamaki *et al.*, 1961).

2.2.2 Toki Granite

The Toki granite occurs to the west of the Naegi granite intruding Paleozoic-Mesozoic sedimentary rocks. It has a circular form, N-S 14 km by E-W 12 km (Fig. 3), and is composed mostly of fine- to medium-grained biotite granite. Granodiorite is present only at the northwestern portion (Suzuki and Ishihara, 1969). Both are magnetite free. Seven samples, two hornblende-bearing, were selected for the chemical analyses. A/CNK ratio of this body (1.09-1.16, Appendix 3), straddling on the S/I type boundary of 1.1, is more aluminous than the Naegi granite. The Toki granitoids have a Rb-Sr whole rock age of 72.3 ±3.9 Ma and initial Sr ratio of 0.7106 ± 0.0001 (Shibata and Ishihara, 1979a).

In contrast to the Naegi granite, the Toki granite contains only a few pegmatites and is not associated with any economic grade of metallic mineralization. Absence of the Nukame granite and drusy pegmatite indicates that the Toki granite crystallized at deeper levels than the Naegi granite.

2.2.3 Ryoke Granitoids

Granitoids distributed to the south of the Naegi and Toki granites around Mt. Sanage (Fig. 3) intrude mainly Jurassic sedimentary accretionary complex rocks with no or low-grade Ryoke metamorphism. The granitoids are the Ryoke I granitoids of Ishihara and Terashima (1977a). The granitoids intrude locally into the Nohi Rhyolites in the north (Yamada and Nakai, 1969), and older granitoids to the south.

These granitoids consist largely of medium- to coarse-grained hornblende-biotite granodiorite and biotite granite. They contain no magnetite. Rare foliated granitoids which occur within in the massive granitoids may be the remnants of older syntectonic granitoids (e.g., nos. 97, 139). Some of the leucocratic biotite granites have been classified as Naegi granite (e.g. Yamada *et al.*, 1974), although they have distinctive chemical characteristics, compared with the Naegi Granite at the type locality (Ishihara and Terashima, 1977a). The leucoratic granites have S-type A/CNK ratios (1.17-1.18, Appendix 3), while the other, more mafic granitoids show generally I-type ratios.

No pegmatite is present, but some aplitic dikelets are observed. No metallic ore deposits are known in and around the Ryoke granitoids. These field observations and the wide exposure of the Ryoke granitoids suggest a deeper level is now exposed in the Ryoke Belt.

3. Analytical Results

3.1 Shirakawa Area

3.1.1 Volcanic rocks

The Nohi Rhyolites analyzed in the Oshirakawa-Hirase area (Fig. 1) have SiO_2 contents of 68.4 -76.6 percent (average 70.3 %, n=6, Appendix 1). Granitoids of the same area including the Mihoro, Hirase (only those from surface) and Fukushima-dani plutons have a similar range from 68.0 to 76.4 percent but are different on average (73.4 %, n=11, Appendix 2). Thus, the granitoids became more silicic than the volcanic rocks. In the Harker's diagram though not shown here, the granitoids are also richer than the rhyolites in Al_2O_3, Na_2O, TiO_2, MgO but lesser in K_2O and total Fe_2O_3.

The Nohi Rhyolites at the eastern margin of the Hirase pluton has experienced "contact" hydrothermal alteration. Chemical compositions of the unaltered rhyolites (nos. 64, 65, 66, 67, average SiO_2 73.8%, n=4) and altered rhyolites (nos. 71, 72, 94, 95 161, average SiO_2 74.9%, n=6) can be summarized as follows:

(1) Ferromagnesian components including total Fe_2O_3, MgO, TiO_2, V, Cr and Ni are strongly decreased in the altered rhyolites, reflecting break down of the original ferromagnesian minerals.

(2)Sr (143 ppm average) and Ba (633 ppm average), are lower in the altered rocks (Sr 28 ppm and Ba 144 ppm, respectively), implying these elements were depleted during recrystallization of the feldspars.

(3) Both Zr (159 ppm) and Hf (4.8 ppm) are slightly increased (220 ppm and 7.0 ppm, respectively) in the altered rocks.

(4) Total LREE (La to Sm) have increased from 131.4 ppm to 223.4 ppm; no clear changes are evident for the HREE (Gd to Lu).

3.1.2 Granitic rocks

Granitoids of the Shirakawa area, i.e., Shirakawa granitoids, have a wide range of SiO_2 content from 60 to 77 percent (Appendix 2). Those with 60-63 percent SiO_2 occur as mafic enclaves or blocks in the Hatogaya body. The Mihoro body is composed of granodiorite with 68-70 percent SiO_2. The Hirase body is characterized by high silica rocks of 71-77 percent SiO_2. The reconnaissance study indicates that the Shirakawa granitoids are rich in Na_2O, as compared with the Naegi-Toki-Ryoke granitoids (Ishihara and Terashima, 1977a). Na_2O apparently decreases with increasing SiO_2 towards 3.6 percent Na_2O of the eutectic minimum (Tuttle and Bowen, 1958). In more details, however, the Shirakawa granitoids can be divided into two groups (Fig. 4):

(A) high Na_2O-low SiO_2 group; Na_2O 4.61 %; SiO_2 68.4 % in average (n=11) and

(B) low Na_2O-high SiO_2 group; Na_2O 3.79 %; SiO_2 75.5 % in average (n=17)(Fig. 4).

Their average compositions are listed in Table 1.

Mafic enclaves and blocks of the Hatogaya body (nos. 86, 88), the granitoids of the attached Aradani body (nos. 83, 84), a small part of the Hirase granitic body (nos. 8, 115) and all of the Mihoro granodiorite body (nos. 6, 68, 69, 70, 73), belong to the high Na_2O group. The low Na_2O group, on the other hand, is composed of all the granitoids of the Hatogaya body (nos. 80, 87, 89, 91, 92, 93), most of the Hirase granitic body (nos. 2, 7, 9, 119, 123; 13, 75, 76, 79, 122), and the Fukushima-dani granitic body

Table 1 Average major and selected trace element compositions of the studied granitoids from the Chubu District.

	Magnetite Series		Ilmenite Series		
	High Na_2O group	Low Na_2O group	Ryoke	Toki	Naegi
Number of analyses	11	17	8	6	8
SiO_2	68.43 %	75.45 %	73.37 %	73.39 %	76.67 %
TiO_2	0.42	0.13	0.18	0.14	0.05
Al_2O_3	15.24	12.97	14.26	14.09	12.67
Total Fe_2O_3	3.27	1.25	1.82	1.74	1.11
MnO	0.11	0.05	0.06	0.06	0.03
MgO	1.00	0.24	0.34	0.26	0.04
CaO	2.75	0.90	1.65	1.33	0.73
Na_2O	4.61	3.79	3.15	3.48	3.52
K_2O	3.07	4.32	4.33	4.25	4.74
P_2O_5	0.13	0.04	0.05	0.06	<0.01
Ig. loss	0.71	0.60	0.73	0.72	0.45
Total	99.75	99.74	99.95	99.92	100.00
Color Index	4.80	1.67	2.40	2.20	1.23
TFe_2O_3/MgO	3.3	5.2	5.4	6.7	27.8
Zn	55.1 ppm	23.5 ppm	33.5 ppm	39.7 ppm	20.9 ppm
Ba	672	502	477	371	76.9
Pb	12.6	13.9	29.1	31.8	28.8
Rb	100	142	182	232	289
Sr	281	98.7	106	99.0	22.6
Rb/Sr	0.36	1.43	1.72	2.34	12.8
Zr	189	103	90.4	112	86.3
Hf	5.2	3.5	3.1	3.7	3.9
Zr/Hf	36.4	29.5	29.2	30.3	22.1
Th	9.4	13.9	19.4	24.0	32.0
U	2.0	4.5	4.0	5.5	9.1
Y	25.7	21.4	37.1	54.7	78.4
REE	160	130	134	140	162

High Na_2O-group: Nos. 86,88,83, 84,8, 115, 6, 68, 69, 70, 73. Low Na_2O-group: Nos.87, 89, 91, 92, 93, 80, 3,7, 9, 119, 123, 13, 75, 76, 79, 122, 58. For the ilmenite-series granitoids, those with SiO_2 higher than 70 % were selected. Ryoke: 105, 110, 109, 114, 94, 60, 145, 70. Toki: T38, T44, T51, T82, T25, T2. Naegi: 175A, 213, 211, 505, 506, 508, 509, 510.

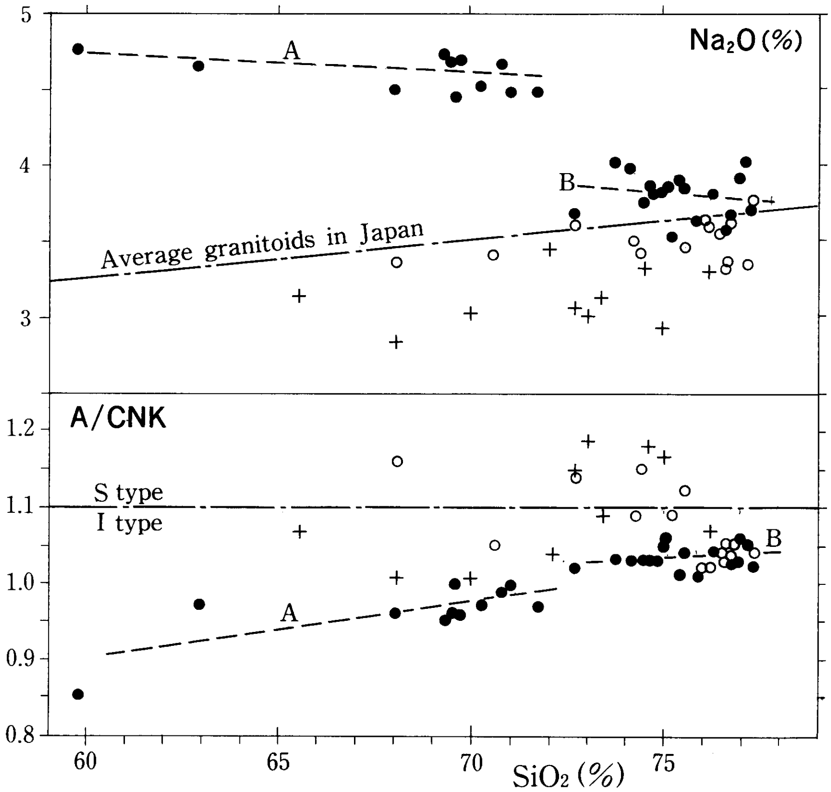

Fig. 4 Two distinctive trends on Na_2O (wt. %) and A/CNK (mol. $Al_2O_3/CaO + Na_2O + K_2O$) of the Shirakawa and Naegi-Toki-Ryoke granitoids. Solid circle, Shirakawa granitoids; open circle, Toki and Naegi granitoids; cross, Ryoke granitoids. Broken line with A and B, general trend for the Shirakawa granitoids. Dotted broken line for Na_2O is average composition of the Japanese granitoids (S. Ishihara, unpublished data), and for A/CNK is S-type and I-type boundary proposed by Chappell and White (1992).

(nos. 58, 61). Both types of granitoids occur together in the Hatogaya body, related to the mingling occurrence of mafic enclaves in this body.

The high Na_2O group is rich in both mafic and calcic components, such as TiO_2, Al_2O_3, Total Fe_2O_3, MnO, MgO, CaO, P_2O_5, Zn and Sr, while the low Na_2O group has higher SiO_2, K_2O, Rb, Th and U. It is considered unusual that the high Na_2O group is also high in Ba, Zr, Y and REE. In Fig. 5, it is evident that Rb is not "constant type" (Ishihara and Terashima, 1977a) but rather shows a weak positive correlation with SiO_2 within each group. Ba is approximately constant in the high Na_2O group, but drops sharply with increasing SiO_2 in the low Na_2O group (Fig. 5). Sr decreases with decreasing CaO and is slightly higher in the Shirakwa granitoids than the Naegi-Toki-Ryoke granitoids.

Athough all the low-Na_2O group granitoids are high in SiO_2, hence in normative ab + or + qz (see Ishihara 1971a), and may be called haplogranite (Bowen abd Tuttle, 1958); yet their Rb/Sr ratios range from as low as 0.5 to 8.7 (Fig. 6). These values are similar to unfractionated I-type haplogranites of the Lachlan Fold Belt (Chappell, 1999). These low Na_2O granites are, therefore, considered a minimum melt of the original magmas, rather than its fractionated products.

REE contents of the high Na_2O group vary from higher in the low SiO_2 end-members (e.g., nos. 86, 88) to lower in the high SiO_2 rocks; the latter are depleted particularly in HREE (Fig. 7A). The high Na_2O granitoids reveal weak negative Eu anomalies. Granodiorites of the Mihoro body show very similar REE patterns to those of Fig. 7A, but no Eu anomaly is observed.

Among the low Na_2O group, granitoids of the Hatogaya body show a wide variation of Eu anomalies and

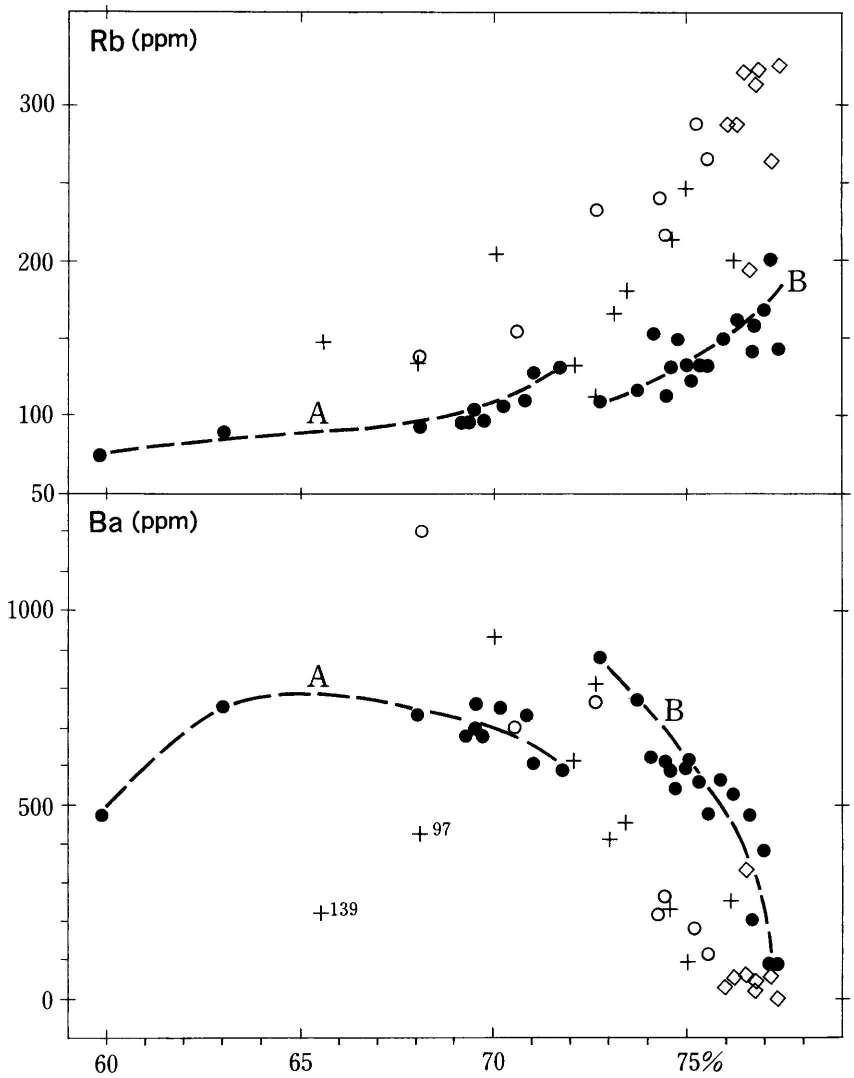

Fig. 5 Rb and Ba vs. SiO_2 diagrams of the studied magnetite-series and ilemenite-series granitoids. Solid circle, Shirakawa granitoids with the high Na_2O trend (A) and low Na_2O trend (B). Open circle, Toki granitoids; open diamond, Naegi granite; cross, Ryoke granitoids. Two granodiorites of the Ryoke Belt (nos. 139, 97) are plotted in low Ba area.

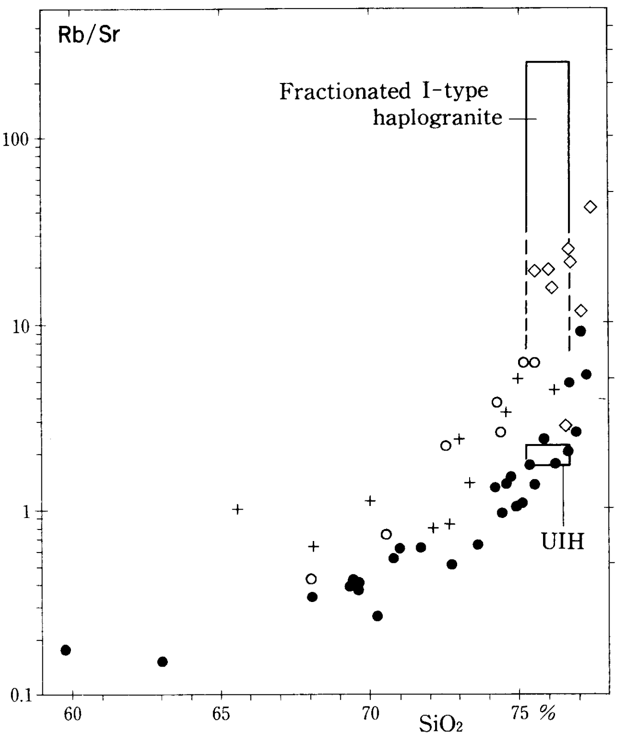

Fig. 6 Rb/Sr ratio vs. SiO_2 diagrams of the studied magnetite-series and ilemenite-series granitoids. Solid circle, Shirakawa granitoids; open circle, Toki granitoids; open diamond, Naegi granite; cross, Ryoke granitoids. Areas of UIH, unfractionated I-type haplogranite and fractionated I-type haplogranite of Chappell (1999).

HREE contents (Fig. 7B). Granitoids occurring in the northern part (nos. 87, 89) have similar LREE patterns to those of the associated monzodiorite but depleted in HREE (compare Figs. 7A and B). Granitoids of the central (nos. 91, 92) and southern parts (nos. 80, 93) reveal a sharp decreasing of both the LREE and Eu, and show strong Eu anomalies.

In the Hirase body, REE patterns of the main biotite granite phase (nos. 13, 75, 76, 79, 122), are similar to those of the low-Na_2O granites of the Hatogaya body (e.g., no. 93). Finer-grained phase of the same body show also similar pattern.

3.2 Naegi-Toki-Sanage Area

The Naegi, Toki and Ryoke granitoids appear to be different in the present erosion level by differential movement along the NE-SW regional faults, and they may also be different in the magma sources. In order to test this hypothesis, some elements pertinent to magmatic fractionation are shown in Table 1. Compared to the Toki granitoids, the Naegi granite is higher in SiO_2, K_2O, Na_2O+K_2O, Fe_2O_3/MgO , Rb, Y, Th, U and REE, but lower in total Fe_2O_3, MgO, CaO, Sr and Ba. Average Rb/Sr ratios are 12.8 for the Naegi granite, versus 2.3 for the Toki granitoid. Because of their depleted MgO, the average total Fe_2O_3/MgO ratio is much higher in the Naegi granite (27.8) than in the Toki granite (6.7). Thus, these parameters indicate that the Naegi granite is much more

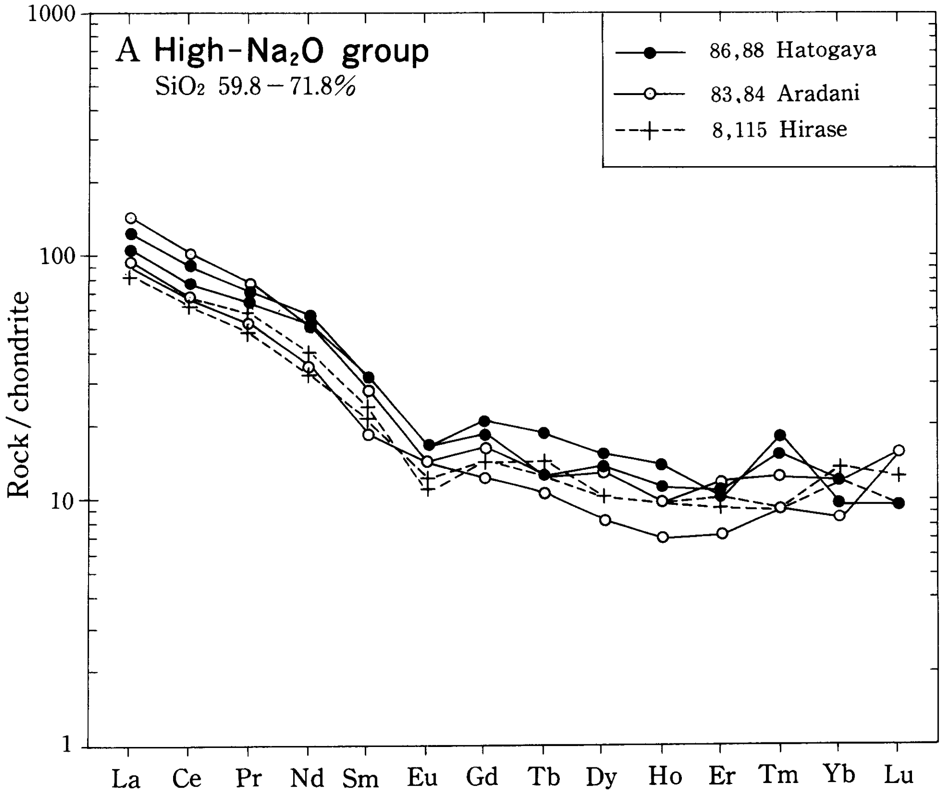

Fig. 7A Representative REE patterns of the Shirakawa granitoids, Chubu District.

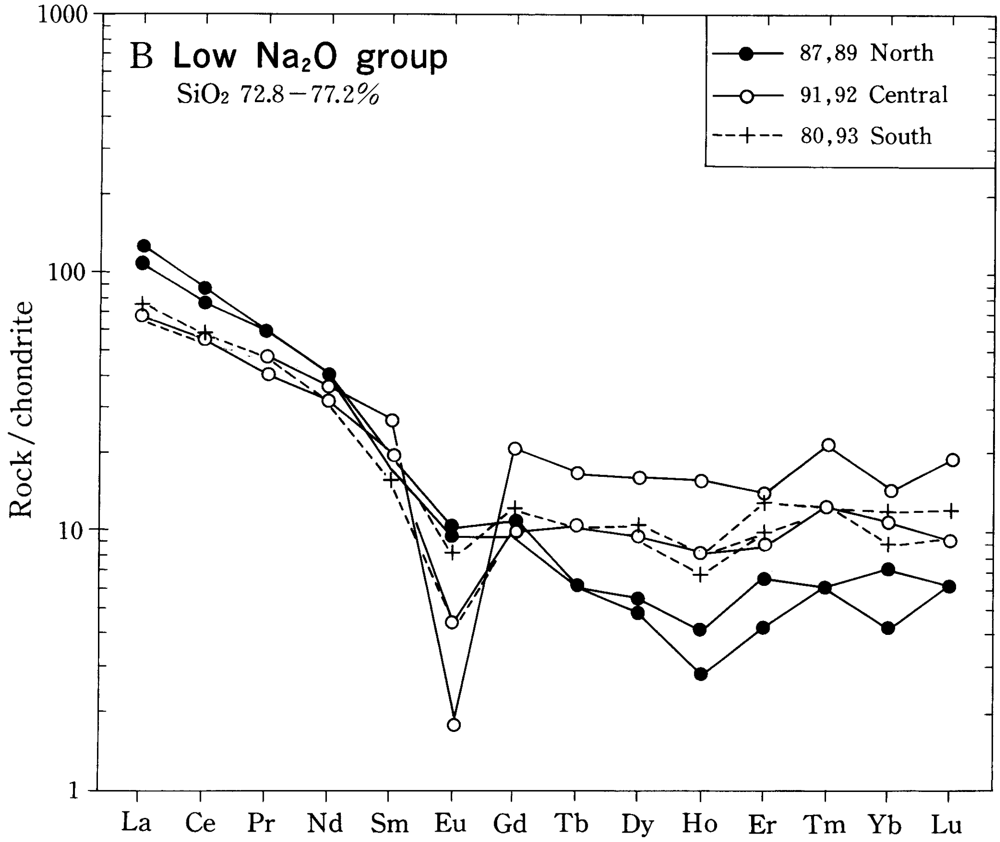

Fig. 7B Representative REE patterns of the Shirakawa granitoids, Chubu District.

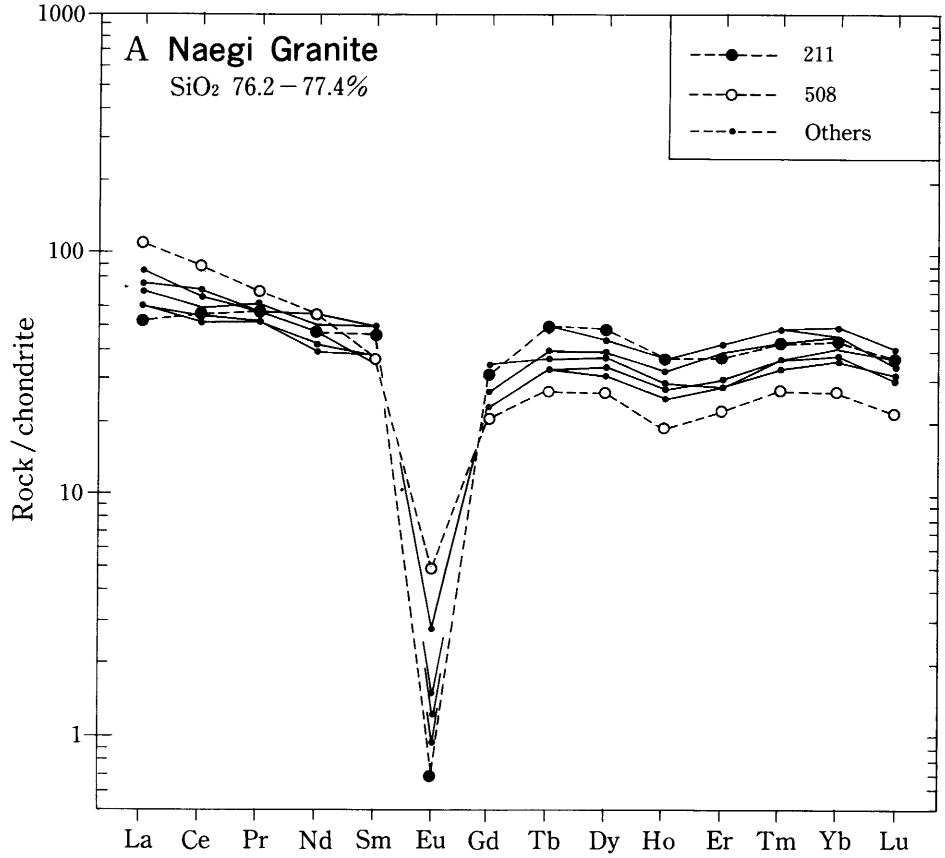

Fig. 8A Representative REE patterns of the Naegi and Toki granitoids, Chubu District.

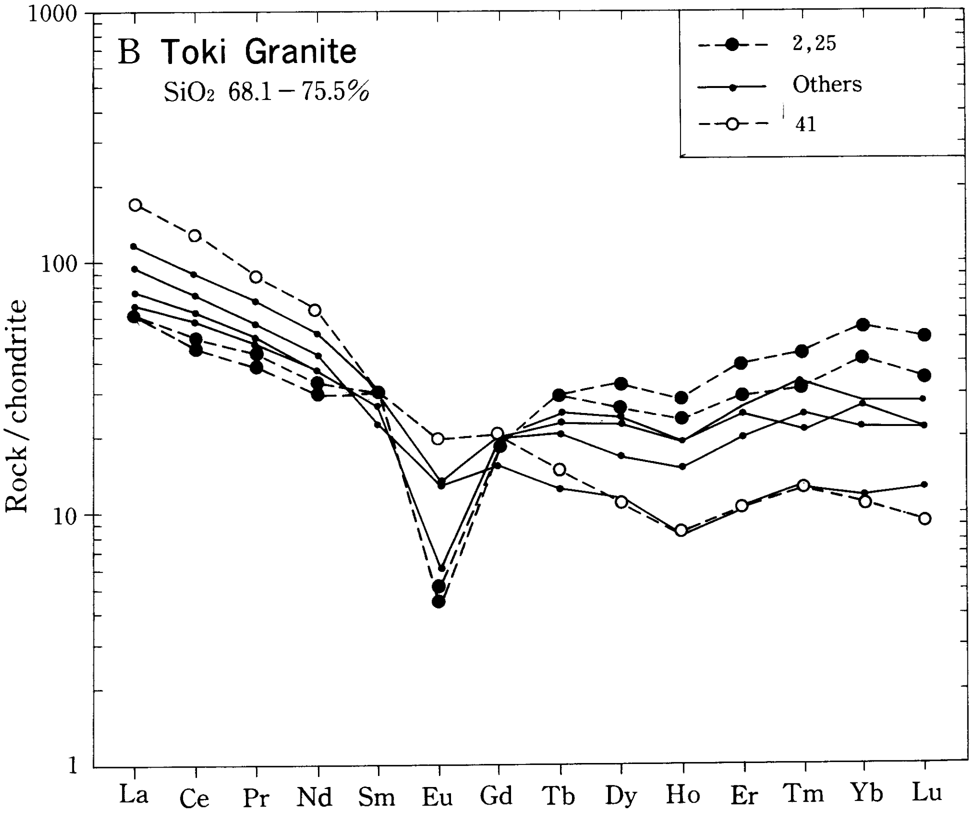

Fig. 8B Representative REE patterns of the Naegi and Toki granitoids, Chubu District.

fractionated than the Toki granite.

Similar variations to those observed between the Naegi and Toki granitoids, are also seen between the Toki and the Ryoke granitoids. Amongst the three granitoids, contents of TiO_2, total Fe_2O_3, MgO, Al_2O_3, CaO, Ba, Sr are highest, and those of Na_2O (Fig.5), Rb, Th, U, REE are the lowest in the Ryoke granitoids. Two samples of the Ryoke granitoids have much lower Ba content (nos. 97, 139, Fig. 5), and may belong to xenolithic block of the older foliated granodiorites generated from different source materials.

REE patterns of the Naegi granite (Fig. 8A) are flat implying high concentration of HREE with strong Eu anomaly, similar to strongly fractionated I-type granite, e.g., the Caboniferous I-type granites of North Queenland (Champion and Chappell, 1992), and to A-type granites of the Lachlan Fold Belt (King *et al.*, 1997) and Zhejiang Province of China (Charoy *et al.*, 1987). Among eight samples studied, the chilled margin phase of "Nukame" granite (no. 211) is most depleted in Eu and highest in Rb/Sr ratio (40.5, Appendix 3), implying plagioclase fractionation. In the Toki granite, hornblende-bearing phases (e.g., nos. 41, 38) and biotite-rich granite (no. 44) are rich in LREE and have no or weak negative Eu anomalies. Other Toki granite samples are rich in HREE and have similar REE pattern to those of the Naegi granite (Fig. 8B).

The Ryoke granitoids have a wide variety of REE patterns, because they include a variety of granitoids in the batholithic unit. Fine-grained biotite granite of stock size, which can be considered equivalent to the Naegi granite (Yamada *et al.*, 1974), has a similar REE pattern to those of the Naegi granite (no. 70), while the other sample (no. 145) is more depleted in both LREE and HREE. The granitoids of nos. 110 and 114 are most depleted in HREE.

4. Discussions

4.1 I type vs. A type

F contents of the Naegi granite are the highest of the Japanese granitoids (Ishihara and Terashima, 1977b). Other elements with high concentration in the Naegi granite are known to be also enriched in A-type granitoids (Collins *et al.*, 1982; Ishihara, 1988; King *et al.*, 1997). Thus, the Naegi granite could possibly be an independent magma of A type. However, Ga is not as rich as A-type granites in the continental regions, like Australia (Fig. 9) and China. As I type becomes strongly fractionated, F, Ga, Y, HREE etc also increase strongly (Champion and Chappell, 1992), such that they in part resemble A-types. Geologically, the Naegi granite occurs at northern margin of the calc-alkaline granitoids of I type. Similar granites are seen along the northern fringe of the Sanyo-Naegi Belt; e.g., biotite granites at Tanokami, Shiga Pref., the Kurashiki area of Okayama Pref. and the Iwakuni

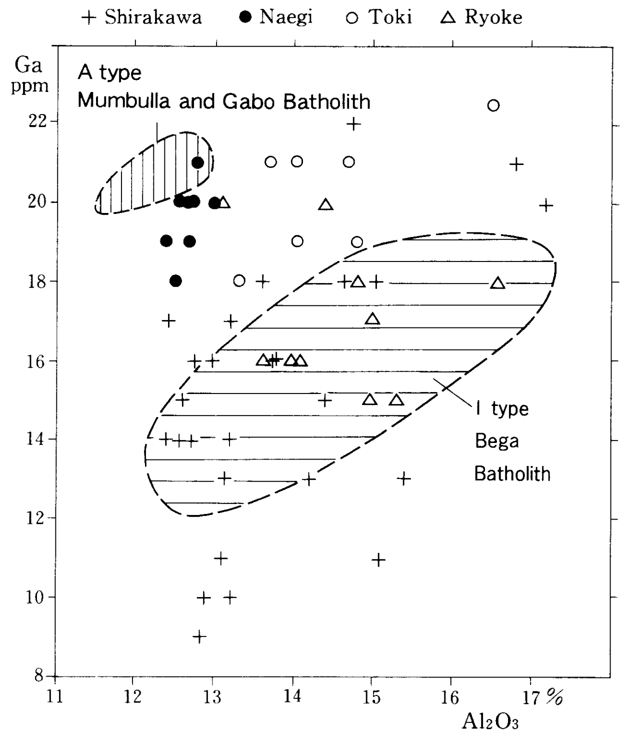

Fig. 9 Ga vs. Al_2O_3 diagram of the studied granitoids and Australian A-type (Mumbulla and Gabo) and I-type (Bega) granites from Collins et al. (1982).

area of Yamaguchi Pref. In the Kurashiki area, the granite occurs at margin of the so-called Hiroshima biotite granite, and the boundary of the two granites is unclear, suggesting that they are cogenetic. The Naegi and Toki granites have had a common I-type source but fractionated in different ways; the Naegi granite is most fractionated and emplaced in the highest level. Thus, it could be fractionated I type ilmenite series.

4.2 Magnetite-series vs. Ilmenite-series Granitoids

Magnetite-series granitoids of the Shirakawa area and ilmenite-series granitoids of the Naegi-Toki-Ryoke area have a wide range of silica contents (58 to 77% and 65 to 77%, respectively). Chemical trends for most major elements are similar in those two granitoid series, except for the Fe_2O_3/FeO ratio and Na_2O content (Ishihara and Terashima, 1977a). As mentioned previously, the Shirakawa granitoids are composed of two groups in terms of Na_2O and SiO_2 contents, and may have different source materials.

The Naegi-Toki granitoids have similar SiO_2 content to the high silica Shirakawa granidoids, but are lower in Na_2O and higher in K_2O. The Ryoke granitoids are much lower in Na_2O content (Fig. 4). Given in relatively high $^{87}Sr/^{86}Sr$ initial ratio, these granitoids are considered to have been generated from different source materials within the continental crust. A Na_2O-rich and K_2O-poor character may be expected in intermediate meta-igneous rocks, while a potassic nature under a reducing atmosphere can be obtained from pelitic and arkossic sedimentary rocks of the source regions. This interpretation is supported by the fact that the magnetite-seires granitoids are mostly meta-aluminous ($A/CNK < 1.0$), while the ilmenite-series rocks are generally per-aluminous ($A/CNK > 1.0$).

Two series of the granitoids are also clearly separated by Y content. The contents are generally lower than 30 ppm in the magnetite-series granitoids, but higher than 30 ppm in the ilmenite-series rocks (Appendices 2, 3). The same is true on the HREE contents. Y and HREE elements are strongly partitioned to garnet, zircon, apatite and titanite, and moderately to hornblende (Pearce and Norry, 1979; Ogasawara, 1989). Thus, the depletion of these elements indicates existence of these minerals, especially of garnet, in the source region for the magnetite-series magmas.

The Hida metamorphic rocks are composed mostly of quartzo-feldspathic gneiss, basic gneiss and calcareous gneiss, associated with lesser amount of pelitic gneiss (Suzuki, 1977). Their bulk composition is a mafic to intermediate one rich in the ferromagnesian components, CaO and Na_2O (Nozawa *et al.*, 1975, 1981; Suzuki, 1975, 1977). These rocks are intruded by magnetite-series Triassic-Jurassic granodiorite and granite and lesser diorites. Their chemical characteristics correspond to those of the Shirakawa granitoids. Some older, gray granitoids occur close to the east of the Shirakawa granitoids. Low Bougeur anomalies are widely present in the Hida metamorphic terrane (Komazawa *et al.*, 1999), indicating that these metamorphic and igneous or similar rocks continue to the depth. The high Na_2O – low SiO_2 and meta-aluminous initial magma and low Na_2O- high SiO_2 initial magma for Shirakawa granitoids could have generated from igneous rocks similar to the present constituents of the Hida metamorphic Belt.

The Mino sedimentary terrane, on the other hand, is an accretionary complex of Jurassic fore-arc sediments. Sandstone, shale, chert and their metamorphic equivalents occur dominantly associated with some limestones and ocean floor basalt (Nakai *et al.*, 1985; Wakita, 2000). Their bulk composition is supposed to be dominantly sandstone, then shale and less chert, thus having high K_2O and Al_2O_3 but low Na_2O contents and a low Fe_2O_3/FeO ratio. These characteristics are also seen in the Naegi-Toki and Ryoke granitoids, implying that the accretionary complex continues to depth. The Ryoke granitoids, however, consist of both hornblende-biobite and biotite mineral asssemblages. Thus, some I-type components are necessary for the source region, which could have been brought as basaltic magmas (Ishihara, 2001). The studied granitoids are considered to reflect the chemical compositions of the immediate basement rocks they were found in.

5. Conclusions

Magnetite-series granitoids of the Shirakawa area are divided into high Na_2O and low Na_2O groups. Each group appears to have its own magma source. Monzodiorite-granodiorite of the Shirakawa granitoids may have originated from mafic and intermediate igneous protoliths containing garnet. Similarly mafic enclaves and granodiorite of the high Na_2O group were derived from mafic igneous protoliths. Biotite granites of low Na_2O group were most likely derived from an igneous source of intermediate composition, similar to those of the Hida metamorphic belt.

The Naegi-Toki-Ryoke granitoids were generated from continental materials, most probably the sedimentary components of the Mino terrane, but also including some igneous-source components. The sedimentary/mafic igneous ratios of the source materials may be different between the Naegi-Toki granitic area and the Ryoke granitic area. The chemical difference between the Naegi and Toki granitoids may be attributed to the degree of fractionation and the depth of emplacement.

Acknowledgements: The chemical analyses of this work was done with guidance of Shigeko Togashi (XRF) and Noboru Imai (ICP-MS) during Chengyu Wu stayed at the Geological Survey of Japan between 1992 and 1995 under the STA post-D. Sc. Fellowship. The authors acknowledge B.W. Chappell for his continued discussion on granite geneses and D. C. Champion for his critical reviewing of the original manuscript.

References

Champion, D. C. and Chappell, B. W. (1992) Petrogenesis of felsic I-type granites: An example from northern Queensland. *Trans. Royal Soc. Edingburgh: Earth Sci.*, **83**, 115-126.

Chappell, B. W. (1999) Aluminium saturation in I- and S-type granites and the characterization of fractionated haplogranites. *Lithos*, **46**, 535-551.

Chappell, B. W. and White, A. J. R. (1992) I- and S-type granites in the Lachlan fold Belt. *Trans. Royal Soc. Edingburgh: Earth Sci.*, **83**, 1-26.

Charoy, B., Couturie, J.P., Raimbault, L. and Liu, Y. (1987) The Suzhou granite complex (East China): Evolution from granite to biotitite with consequent Zr and REE mineralization. Abst. Intern. Sym. *"Petrogenesis and Mineralizations of Granitoids"*. Inst. Geochem. (Guiyang), 22-23.

Collins, W.J., Beams, S.D., White, A.J.R. and Chappell, B.W. (1982) Nature and origin of A-type granites with particular reference to southwestern Australia. *Contrib. Mineral. Petrol.*, **80**, 189-200.

Ishihara, S. (1971a) Major molybdenum deposits and related granitic rocks in Japan. Rept. *Geol. Surv. Japan*, no. 239, 178 p. (in Japanese with English abstract).

Ishihara, S. (1971b) Modal and chemical compositions of the granitic rocks related to the major molybdenum and tungsten deposits in the Inner Zone of Southwest Japan. *Jour. Geol. Soc. Japan*, **77**, 441-452.

Ishihara, S. (1973) The Mo-W metallogenic provinces and the related granitic provinces. *Mining Geol.*, **23**, 13-32 (in Japanese with English abstract).

Ishihara, S. (1984) Granitoid series and Mo/W-Sn mineralization in East Asia. Rept. *Geol. Surv. Japan*, no. 263, 173-208.

Ishihara, S. (1988) A-type granite and REE ore deposits. *Chishitsu News*, no. 409, 6-24 (in Japanese).

Ishihara, S. (1990) The Inner Zone batholith vs. the Outer Zone batholith in Japan; Evaluation from their magnetic susceptibility. In M. Shimizu & G. Gastil ed., Recent *Advances in Concepts Concerning Zoned Plutons in Japan and Southern and Baja California*. The Univ. Museum, Univ. Tokyo, Nature & Culture, 2, 21-34.

Ishihara, S. (2001) Tectonic setting of S-type granitoids in Japan. *Lithos* (submitted).

Ishihara, S. and Terashima, S. (1977a) Chemical variation of the Cretaceous granitoids across southwestern Japan -Shirakawa-Toki-Okazaki transection - *Jour. Geol. Soc. Japan*, **83**, 1-18.

Ishihara, S. and Terashima, S. (1977b) Chlorine and fluorine contents of granitoids as an indicator for base metal and tin mineralizations. *Mining Geol.*, **27**, 191-199.

Kawata, K. (1961) Explanatory text of the geological map of Japan. "Tsukechi". Scale 1:50,000, *Geol. Surv. Japan*. 69 p. (in Japanese with English abstract).

Koido, Y. and Yamada, N. (1999) Nohi Rhyolites. In Excursion Guidebook, 106th Ann. Mtg. *Geol. Soc. Japan* (Nagoya), 47-64 (in Japanese).

King, P.L., White, A.J.R., Chappell, B.W. and Allen, C.M. (1997) Characterization and origin of aluminous A-type granites from the Lachlan Fold Belt, southeastern Australia. *Jour. Petrol.* 38, 371-391.

Komazawa, M., Hiroshima, T., Ishihara, T., Murata, Y., Yamazaki, T., Joshima, M., Makino, M., Morijiri, R., Shichi, R., Kishimoto, K. and Kikawa, E. (1999) Gravity anomaly of Japan (Bouguer anonalies), Scale

1:1,000,000, *Geol. Surv. Japan*. 14 p.

Koseki, K. and Matsubara, H. (1961) Uraniferous pegmatite deposits in Japan. In Natural Occurrence of Uranium in Japan, Pt. 1. *Rept. Geol. Surv.* Japan, no.190, 13-26 (in Japanese with English abstract).

Nakai, Y., Takeuchi, A., Suganuma, T., Ohta, S., Sakamoto, E., Yamamoto, N. and Uchida, Y. (1985) Physiography and geology of Okazaki city. History of Okazaki City, new edition. Nature 14, 209 p. (in Japanese).

Nozawa, T., Kawata, K. and Kawai, M. (1975) Geology of the Hida-Furukawa District. Quadrangle Series, Scale 1:50,000, *Geol. Surv. Japan*. 79 p.

Nozawa, T., Sakamoto, T., Kano, T. and Inazuki, T. (1981) Geology of the Shirokimine Deistrict. Quadrangle Series, Scale 1:50,000, *Geol. Surv. Japan*. 85 p.

Ogasawara, M. (1989) Geochemistry of rare-earth elements. *Mining Geol.*, **39**, 166-176 (in Japanese with English abstract).

Onishi, A., Matsuki, M. and Kobayashi, N. (1973) Geology of the Hirase molybdenum mine area, Gifu Prefecture. *Mining Geol.*, **23**, 119-136 (in Japanese with English abstract).

Pearce, J. A. and M. J. Norry (1979) Petrogenetic implications of Ti, Zr, Y and Nb variations in volcanic rocks. *Contrib. Mineral. Petrol.*, **69**, 33-47.

Sakamaki, Y., Hamachi, T. and Igarashi, T. (1961) Granitic rocks and related uraniferous ore deposits in Naegi District. In Natural Occurrence of Uranium in Japan pt. 1, *Rept. Geol. Surv.* Japan, no. 190, 56-68 (in Japanese with English abstract).

Shibata, K. and Ishihara, S. (1979) Rb-Sr whole-rock and K-Ar mineral ages of granitic rocks in Japan. *Geochem*. J., **13**, 113-119.

Suzuki, M. (1975) On the petrochemical character of the pelitic gneiss from the southwestern part in the Hida metamorphic belt, central Japan. *Jour. Sci. Hiroshima Univ.*, Ser. C, 7, 133-148.

Suzuki, M. (1977) Polymetamorphism in the Hida metamorphic belt, central Japan. *Jour. Sci. Hiroshima Univ.*, Ser. C, 7, 217-296.

Suzuki, Y. and Ishihara, S. (1969) Modal compositions of granitic plutons of Toki-Okazaki region, central Japan. In Natural Occurrence of Uranium in Japan, Pt. 2, *Rept. Geol. Surv. Japan*, no. 232, 155-168 (in Japanese with English abstract).

Tuttle, O.F. and Bowen, N.L. (1958) Origin of the granite in the light of experimental studies in the system $NaAlSi_3O_8$-$KaAlSi_3O_8$-SiO_2-H_2O. *Geol. Soc. America, Mem*. **74**, 158 p.

Wakita, K. (2000) Melanges of the Mino terrane. *Mem. Geol. Soc. Japan*, no. 55,145-163 (in Japanese with English abstract).

Wu, C.-Y. and Ishihara, S. (1994) REE geochemistry of the southern Thailand granites. *Jour. SE Asian Earth Sci.*, **10**, 81-94.

Wu, C.-Y., Bai, G., Yuan, Z.-X., Nakajima, T. and Ishihara, S. (1993) Proterozoic metamorphic rock-hosted Zr, Y and HREE mineralization in the Dabie Mountain area, central China. *Intern. Geol. Review*, **35**, 898-919.

Yamada, N. (1977) Nohi Rhyolite and associated granitic rocks. In Yamada, N., Nozawa, T., Hayama, Y. and Yamada, T. ed. Mesozoic Felsic Igneous Activity and Related Metamorphism in Central Japan - from Nagoya to Toyama-. Guidebook Exc. 4, 33-60, *Geol. Surv. Japan*.

Yamada, N. (1989) Late Cretaceous Ena cauldron found in the southermost part of the Nohi rhyolitic mass, central Japan. *Assoc. Geol. Collab. Japan*, Mongraph no. 36, 21-33 (in Japanese with English abstract).

Yamada, N. and Nakai, Y. (1969) Geologic relations between the Nohi Rhyolites and the so-called Ryoke granites in central Japan. *Mem. Geol. Soc. Japan*, 4, 51-60 (in Japanese with English abstract).

Yamada, N., Katada, M., Hayama, Y., Yamada, T., Nakai, Y., Kutsukake, T. Suwa, K. and Miyagawa, K. (1974) Geological map of the Ryoke belt, central Japan. Miscel. Map Ser. 18, *Geol. Surv. Japan*.

Received July 16, 2001
Accepted December 20, 2001

Appendix 1 Major and trace element contents of the Nohi Rhyolites from the Shirakawa area.

Location	Fresh Rhyolite						Altered Rhyolite				
Sample No.	67RS-60	67RS-64	67RS-65	67RS-66	67RS-67	67RS-78	67RS-71	67RS-72	67RS-94	67RS-95	67RS-161
SiO_2 (%)	58.57	72.93	75.20	74.81	72.09	68.39	72.68	75.33	75.61	74.44	76.62
TiO_2	0.92	0.21	0.20	0.14	0.23	0.38	0.10	0.08	0.09	0.10	0.10
Al_2O_3	16.52	14.66	13.17	12.78	13.88	14.68	13.61	12.77	12.36	13.33	14.24
TFe_2O_3	6.96	2.40	1.90	1.70	2.53	2.98	1.57	1.34	1.81	2.19	0.76
MnO	0.14	0.06	0.04	0.04	0.08	0.08	0.10	0.06	0.07	0.04	0.02
MgO	2.74	0.49	0.30	0.15	0.59	0.88	0.02	0.01	0.06	0.03	0.03
CaO	6.40	1.54	1.05	1.00	1.56	2.46	0.58	0.34	0.41	0.24	0.07
Na_2O	2.92	2.66	1.95	3.39	3.43	4.05	4.02	3.58	3.21	2.17	0.92
K_2O	3.34	4.26	4.77	4.28	3.98	3.63	5.13	5.10	4.46	5.83	5.59
P_2O_5	0.30	0.04	0.04	0.03	0.05	0.10	0.01	0.01	0.01	0.02	0.02
LOI	1.19	1.25	1.11	0.78	0.88	0.69	1.26	0.95	1.11	1.02	0.65
Total	100.00	100.50	99.73	99.11	99.30	98.32	99.08	99.57	99.20	99.40	99.02
V (ppm)	178	20	13	6	21	37	3	NA	NA	NA	NA
Cr	92	39	38	45	33	24	22	NA	NA	NA	NA
Ni	16	11	11	8	11	6	8	NA	NA	NA	NA
Zn	127	39	28	37	151	47	34	25	53	211	49
Ga (XRF)	20	16	17	22	19	17	16	13	19	18	22
Rb (XRF)	108	170	179	139	140	118	169	182	156	246	270
Sr (XRF)	446	142	120	119	189	255	42	26	22	25	24
Y (XRF)	26.7	39.4	41.1	28.8	28.7	24.4	35.7	32.4	33.4	38.4	37.6
Zr (XRF)	174	172	165	149	148	162	235	210	192	232	230
Nb	10	12	13	12	12	11	15	12	14	15	16
Sn	3.4	4.2	3.7	2.1	4.9	1.2	3.9	2.2	3.3	3.3	3.7
Cs	7.6	10.4	8.5	5.0	6.4	2.5	1.8	2.2	2.1	6.2	8.7
Ba (XRF)	934	562	674	636	658	789	151	108	112	161	188
La	25	41	37	31	31	33	59	44	46	61	59
Ce	52	80	72	60	62	65	112	88	95	115	118
Pr	6.5	9.4	9.0	6.5	7.2	7.2	12.6	10.1	10.7	13.0	13.7
Nd	25	34	32	23	26	26	47	38	38	46	49
Sm	4.5	7.6	6.9	4.6	5.2	4.5	8.7	8.6	6.7	7.0	7.8
Eu	1.33	0.77	0.87	0.54	0.57	0.95	0.41	0.30	0.20	0.52	0.29
Gd	4.2	6.9	7.0	4.4	5.1	3.7	7.0	6.8	5.9	6.8	7.2
Tb	0.7	0.9	1.1	0.6	0.7	0.6	1.0	1.0	1.0	1.2	1.1
Dy	3.1	6.2	6.4	3.5	4.3	3.7	6.4	5.8	6.0	6.4	6.6
Ho	0.7	1.1	1.1	0.7	0.7	0.7	0.9	1.0	1.0	1.0	1.1
Er	2.4	4.5	4.9	2.9	3.3	2.0	4.0	3.4	2.7	3.0	3.2
Tm	0.5	0.9	0.9	0.5	0.5	0.4	0.7	0.7	0.6	0.6	0.7
Yb	2.0	4.5	2.7	2.2	2.7	2.8	3.3	4.8	3.8	3.7	4.3
Lu	0.3	0.6	0.8	0.5	0.7	0.4	0.8	0.6	0.5	0.4	0.6
Hf	4.5	5.3	5.2	4.2	4.3	4.9	6.4	8.0	5.8	7.3	7.4
Ta	0.7	1.5	1.1	0.9	0.9	0.9	1.0	1.3	1.2	1.3	1.5
Pb	23	20	22	18	47	17	46	27	24	27	27
Th	9.7	17.7	16.8	12.7	14.5	12.0	19.0	18.0	17.7	17.4	19.9
U	2.0	3.8	3.9	2.8	3.1	2.3	4.6	3.4	3.8	3.6	3.9
REE	154.5	238.0	224.1	169.4	178.8	175.9	298.8	246.1	251.4	303.3	309.4
Sm/Nd	0.18	0.22	0.22	0.20	0.20	0.17	0.19	0.22	0.18	0.15	0.16
Rb/Sr	0.2	1.2	1.5	1.2	0.7	0.5	4.0	7.0	7.1	9.8	11.3
Th/U	4.8	4.7	4.3	4.5	4.8	5.3	4.1	5.2	4.6	4.8	5.2
10000Ga/Al	2.34	2.07	2.43	3.18	2.54	2.13	2.28	1.93	2.86	2.58	2.92
Y/Nb	2.8	3.2	3.2	2.5	2.5	2.2	2.4	2.8	2.3	2.6	2.4
Nb/Ta	14.5	8.6	11.6	12.4	12.9	12.6	14.7	8.7	12.0	11.6	10.6
Zr/Hf	39.0	32.5	31.6	35.7	34.3	33.3	36.6	26.4	33.1	32.0	31.0
A/CNK	0.82	1.24	1.28	1.06	1.09	0.97	1.03	1.06	1.14	1.29	1.85
TFeO/MgO	2.3	4.5	5.8	10.0	3.9	3.1	71.4	121.8	27.4	79.6	23.0

Appendix 2 Major and trace element contents of the Shirakawa granitoids.

Location	North Hatogaya						South Hatogaya		Aradani	
Sample No.	67RS-86	67RS-87	67RS-88	67RS-89	67RS-91	67RS-92	67RS-80	67RS-93	67RS-83	67RS-84
SiO_2 (%)	62.96	72.78	59.84	73.73	76.73	77.17	75.56	77.00	70.80	70.26
TiO_2	0.49	0.24	0.84	0.21	0.07	0.06	0.14	0.09	0.33	0.33
Al_2O_3	17.18	13.72	16.80	13.68	12.66	12.71	13.20	12.63	14.65	14.72
TFe_2O_3	4.62	1.85	6.18	1.64	0.89	0.87	1.33	1.07	2.64	2.55
MnO	0.12	0.04	0.23	0.05	0.04	0.05	0.05	0.05	0.10	0.08
MgO	1.33	0.46	2.37	0.47	0.11	0.12	0.23	0.17	0.66	0.74
CaO	3.87	1.60	5.30	1.27	0.55	0.46	1.02	0.64	1.95	2.26
Na_2O	4.64	3.67	4.77	4.01	3.67	4.02	3.86	3.58	4.68	4.56
K_2O	2.82	4.11	2.09	4.09	4.82	4.31	4.19	4.52	3.35	3.33
P_2O_5	0.24	0.07	0.27	0.07	0.01	0.01	0.04	0.02	0.10	0.11
LOI	1.18	0.63	1.04	0.92	0.19	0.36	0.40	0.51	0.38	0.52
Total	99.45	99.17	99.73	100.14	99.74	100.14	100.02	100.28	99.64	99.46
V (ppm)	46	22	119	13	3	<2	9	5	23	29
Cr	<4	16	20	<4	6	7	18	17	<4	27
Ni	6	4	8	2	6	6	7	6	2	7
Zn	56	32	85	26	28	14	30	27	62	67
Ga (XRF)	20	16	21	16	14	16	17	15	18	21
Rb (XRF)	75	109	73	116	158	200	132	168	109	104
Sr (XRF)	492	224	427	188	34	23	102	67	207	246
Y (XRF)	27.9	9.0	29.4	11.5	20.3	32.5	23.2	19.5	26.5	20.3
Zr (XRF)	267	140	169	139	90	75	103	87	183	171
Nb	8	5	12	6	9	13	12	10	12	9
Sn	2.1	0.6	2.7	0.5	1.9	2.4	0.9	1.9	2.3	1.4
Cs	1.1	0.5	0.8	0.9	1.7	3.1	1.0	1.3	1.4	1.1
Ba (XRF)	747	876	466	772	200	86	471	378	726	747
La	38	39	32	34	21	21	24	21	44	29
Ce	75	71	63	64	45	46	48	43	82	54
Pr	8.8	7.4	8.1	7.3	5.0	5.8	5.9	5.3	9.3	6.3
Nd	34	24	32	24	19	22	20	18	30	21
Sm	6.2	3.5	6.5	3.8	3.7	5.2	3.8	3.2	5.4	3.6
Eu	1.22	0.71	1.22	0.75	0.32	0.13	0.60	0.33	1.08	1.04
Gd	4.8	2.9	5.5	2.5	2.7	5.4	3.2	2.8	4.2	3.2
Tb	0.6	0.3	0.9	0.3	0.5	0.8	0.5	0.5	0.6	0.5
Dy	4.4	1.6	4.9	1.8	3.2	5.2	3.4	3.1	4.1	2.6
Ho	0.8	0.2	1.0	0.3	0.6	1.1	0.6	0.5	0.7	0.5
Er	2.3	0.9	2.2	1.4	1.9	2.9	2.8	2.1	2.4	1.5
Tm	0.5	0.2	0.6	0.2	0.4	0.7	0.4	0.4	0.4	0.3
Yb	2.5	0.9	2.0	1.5	2.3	3.0	2.5	1.9	2.5	1.8
Lu	0.3	0.2	0.3	0.2	0.3	0.6	0.4	0.3	0.5	0.3
Hf	6.7	3.0	4.7	4.0	2.9	3.8	3.8	2.6	5.7	4.7
Ta	0.6	0.4	0.7	0.6	1.2	2.1	0.9	0.9	0.7	0.5
Pb	6	8	5	8	17	15	15	17	13	12
Th	6.7	8.4	5.0	11.0	15.4	25.6	16.2	16.9	11.7	8.9
U	1.9	1.2	1.5	2.4	3.4	4.8	3.4	2.7	2.2	1.6
REE	206.9	162.0	189.4	153.5	126.0	151.6	139.2	121.7	214.0	146.8
Sm/Nd	0.18	0.14	0.21	0.16	0.19	0.24	0.19	0.18	0.18	0.17
Rb/Sr	0.2	0.5	0.2	0.6	4.6	8.7	1.3	2.5	0.5	0.4
Th/U	3.5	7.1	3.3	4.6	4.5	5.4	4.8	6.3	5.4	5.7
10000Ga/Al	2.20	2.16	2.41	2.18	2.07	2.39	2.47	2.29	2.29	2.70
Y/Nb	3.3	1.9	2.5	1.9	2.3	2.4	1.9	1.9	2.3	2.3
Nb/Ta	14.6	12.1	17.4	9.6	7.6	6.3	13.6	11.8	15.6	17.3
Zr/Hf	40.0	46.5	35.9	34.4	31.5	19.6	27.0	32.8	32.0	36.8
A/CNK	0.97	1.02	0.85	1.03	1.03	1.05	1.04	1.06	0.99	0.97
TFeO/MgO	3.2	3.7	2.4	3.2	7.4	6.6	5.3	5.7	3.6	3.1

Appendix 2 Continued.

Location	Hirase									
Sample No.	67RS-115	66RS-2	66RS-7	66RS-9	67RS-119	67RS-123	66RS-8	66RS-13	67RS-75	67RS-76
SiO_2 (%)	71.04	76.70	75.90	75.37	77.34	74.59	71.75	74.96	75.07	76.32
TiO_2	0.27	0.10	0.10	0.11	0.05	0.14	0.24	0.17	0.17	0.12
Al_2O_3	14.39	12.37	12.43	12.55	12.57	12.91	14.21	13.10	13.14	12.93
TFe_2O_3	2.26	0.76	0.83	1.14	0.74	1.36	1.91	1.24	1.50	1.23
MnO	0.09	0.04	0.05	0.06	0.03	0.06	0.08	0.06	0.06	0.06
MgO	0.64	0.11	0.17	0.10	0.03	0.26	0.53	0.36	0.29	0.21
CaO	1.90	0.74	0.74	0.77	0.54	0.91	2.01	1.05	0.93	0.84
Na_2O	4.48	3.57	3.63	3.89	3.70	3.86	4.49	3.83	3.86	3.80
K_2O	3.32	4.44	4.58	4.33	4.81	4.22	3.27	3.95	4.07	4.28
P_2O_5	0.08	0.02	0.02	0.03	0.01	0.03	0.07	0.05	0.05	0.02
LOI	0.92	0.66	0.72	0.86	0.38	1.23	0.89	0.56	0.42	0.48
Total	99.40	99.51	99.17	99.21	100.20	99.57	99.45	99.33	99.56	100.29
V (ppm)	17	3	4	7	<2	7	16	8	9	6
Cr	24	23	22	30	23	29	18	14	9	7
Ni	6	5	6	6	7	6	4	5	3	4
Zn	35	15	12	23	13	18	25	14	34	23
Ga (XRF)	15	17	14	14	9	10	13	11	10	16
Rb (XRF)	127	141	150	132	143	130	131	132	121	161
Sr (XRF)	211	71	66	80	28	97	215	133	120	94
Y (XRF)	25.2	23.1	21.9	15.4	17.9	19.8	17.9	20.1	22.7	23.4
Zr (XRF)	148	84	96	110	56	102	136	112	112	88
Nb	5	17	12	7	9	9	8	9	9	5
Sn	1.3	1.6	1.1	0.8	1.6	1.2	1.5	1.2	0.9	1.6
Cs	1.9	0.9	1.0	1.4	1.5	1.5	1.7	1.2	0.8	3.7
Ba (XRF)	602	474	558	555	88	582	583	589	607	524
La	26	29	27	30	16	33	28	36	30	22
Ce	51	55	54	60	37	67	56	72	54	46
Pr	6.0	6.5	6.2	6.6	4.6	7.8	6.8	8.3	7.0	5.4
Nd	20	21	20	21	17	25	24	29	25	19
Sm	4.2	3.8	3.5	3.2	3.2	5.1	4.6	4.6	4.6	3.9
Eu	0.89	0.53	0.49	0.50	0.39	0.63	0.82	0.58	0.64	0.52
Gd	3.7	3.1	3.2	3.0	2.4	4.3	3.7	3.6	4.1	3.5
Tb	0.7	0.5	0.5	0.4	0.6	0.8	0.6	0.7	0.7	0.6
Dy	3.3	3.9	3.3	2.3	3.4	3.9	3.4	3.6	4.0	3.3
Ho	0.7	0.7	0.6	0.4	0.6	0.6	0.7	0.7	0.7	0.7
Er	2.2	3.1	2.2	1.6	2.6	2.5	2.0	2.3	2.9	2.7
Tm	0.3	0.4	0.5	0.2	0.4	0.4	0.3	0.4	0.5	0.4
Yb	2.8	3.0	2.4	1.4	2.4	2.3	2.4	2.6	2.5	2.8
Lu	0.4	0.5	0.4	0.3	0.3	0.4	0.3	0.4	0.4	0.4
Hf	4.6	2.9	3.3	3.5	2.2	3.9	4.3	4.5	4.1	3.2
Ta	0.5	1.3	1.1	0.6	1.1	1.2	0.8	1.1	1.1	0.6
Pb	10	14	16	16	20	13	12	13	13	14
Th	9.7	11.9	14.2	10.6	12.8	13.7	10.2	13.4	13.7	12.8
U	2.1	2.9	2.9	2.6	2.9	2.5	2.1	2.5	2.4	3.9
REE	147.3	154.7	146.9	146.9	108.8	173.4	151.5	183.9	159.8	134.9
Sm/Nd	0.21	0.18	0.17	0.15	0.19	0.20	0.19	0.16	0.19	0.20
Rb/Sr	0.6	2.0	2.3	1.7	5.1	1.3	0.6	1.0	1.0	1.7
Th/U	4.7	4.1	4.9	4.0	4.5	5.5	5.0	5.3	5.7	3.3
10000Ga/Al	2.01	2.52	2.16	2.03	1.40	1.47	1.77	1.61	1.50	2.26
Y/Nb	5.2	1.4	1.8	2.3	2.1	2.3	2.2	2.3	2.6	4.3
Nb/Ta	10.6	13.4	10.9	11.8	7.9	7.2	9.9	8.0	7.6	8.8
Zr/Hf	31.9	28.8	28.9	31.1	25.8	26.1	31.6	25.2	27.3	27.8
A/CNK	1.00	1.03	1.01	1.01	1.02	1.03	0.97	1.05	1.06	1.04
TFeO/MgO	3.2	6.3	4.4	10.4	22.4	4.8	3.3	3.1	4.7	5.3

Appendix 2 Continued.

Location	Hirase		Mihoro					Fukushima dani	
Sample No.	67RS-79	67RS-122	66RS-6	67RS-68	67RS-69	67RS-70	67RS-73	67RS-58	67RS-61
SiO_2 (%)	74.47	74.73	69.56	68.04	69.71	69.31	69.49	74.15	76.36
TiO_2	0.16	0.15	0.43	0.49	0.41	0.43	0.40	0.20	0.08
Al_2O_3	13.15	13.11	15.07	15.39	15.04	15.14	15.06	13.62	12.45
TFe_2O_3	1.55	1.37	3.20	3.55	3.01	3.19	2.94	1.84	1.01
MnO	0.05	0.05	0.09	0.10	0.09	0.09	0.08	0.06	0.03
MgO	0.33	0.30	0.96	1.11	0.87	0.94	0.85	0.44	0.05
CaO	1.14	0.95	2.37	3.00	2.52	2.61	2.50	1.19	0.34
Na_2O	3.75	3.82	4.46	4.49	4.69	4.73	4.70	3.98	2.66
K_2O	4.13	4.37	3.16	3.02	3.12	3.09	3.14	4.18	6.24
P_2O_5	0.05	0.04	0.11	0.14	0.12	0.12	0.11	0.05	0.01
LOI	0.68	0.64	0.62	0.59	0.60	0.38	0.73	0.49	0.39
Total	99.46	99.53	100.03	99.92	100.18	100.03	100.00	100.20	99.61
V (ppm)	9	8	36	48	32	38	31	11	5
Cr	23	15	26	12	16	16	10	<4	12
Ni	5	4	6	5	5	6	3	4	7
Zn	29	16	31	46	73	72	58	45	30
Ga (XRF)	14	13	11	13	18	19	19	18	14
Rb (XRF)	116	149	95	91	97	97	103	152	188
Sr (XRF)	128	102	255	279	249	255	257	120	81
Y (XRF)	26.4	24.3	28.3	23.8	28.2	29.1	26.0	33.6	21.6
Zr (XRF)	113	109	210	208	200	198	186	136	103
Nb	6	5	3	3	10	12	10	14	9
Sn	0.9	1.5	3.0	2.2	1.3	1.8	1.4	2.4	1.4
Cs	1.4	1.6	2.4	2.0	1.1	2.1	1.9	2.7	2.3
Ba (XRF)	611	543	759	737	667	667	694	612	736
La	29	26	42	36	35	37	31	32	28
Ce	60	54	81	72	71	74	61	66	57
Pr	6.9	6.1	9.7	8.8	8.2	8.5	7.3	7.6	6.5
Nd	24	20	35	30	29	30	25	26	21
Sm	5.0	4.8	6.0	5.7	4.6	5.1	4.3	4.2	3.3
Eu	0.66	0.65	1.41	1.78	1.43	1.33	1.33	0.65	0.48
Gd	4.6	4.2	5.2	5.6	4.8	4.8	4.1	4.4	3.0
Tb	0.8	0.6	0.9	0.8	0.7	0.7	0.6	0.7	0.6
Dy	4.2	3.1	4.7	4.4	3.9	4.3	3.8	4.4	2.6
Ho	0.7	0.6	0.7	0.7	0.6	0.8	0.6	0.7	0.5
Er	3.2	1.8	2.8	2.7	2.6	3.0	2.5	3.1	2.0
Tm	0.4	0.4	0.4	0.4	0.5	0.6	0.4	0.6	0.5
Yb	3.6	2.8	2.7	2.8	2.4	2.1	2.2	2.7	2.3
Lu	0.5	0.4	0.5	0.4	0.4	0.4	0.3	0.5	0.4
Hf	3.4	4.2	5.3	5.2	4.9	5.8	5.6	4.7	4.3
Ta	0.6	0.5	0.3	0.3	0.8	0.9	0.8	1.2	1.3
Pb	12	11	17	15	15	16	15	15	19
Th	13.2	12.6	10.2	7.8	10.7	11.6	10.6	14.5	18.7
U	3.0	3.3	1.7	1.5	2.2	2.3	2.3	2.8	3.3
REE	169.8	149.4	220.6	194.8	192.6	201.6	169.8	186.2	150.1
Sm/Nd	0.21	0.24	0.17	0.19	0.16	0.17	0.17	0.16	0.15
Rb/Sr	0.9	1.5	0.4	0.3	0.4	0.4	0.4	1.3	2.3
Th/U	4.4	3.9	6.0	5.3	4.8	5.0	4.7	5.2	5.7
10000Ga/Al	2.04	1.83	1.43	1.56	2.20	2.33	2.41	2.47	2.17
Y/Nb	4.5	5.4	8.8	8.4	2.7	2.5	2.6	2.4	2.4
Nb/Ta	9.5	9.6	9.7	10.4	13.5	13.7	13.0	11.3	7.2
Zr/Hf	33.1	25.8	39.9	39.9	40.5	34.1	33.5	29.2	24.0
A/CNK	1.03	1.03	1.00	0.96	0.96	0.95	0.96	1.03	1.06
TFeO/MgO	4.3	4.2	3.0	2.9	3.1	3.1	3.1	3.8	19.5

Appendix 3 Major and trace element contents of the Toki, Naegi and Ryoke granitoids.

	Toki									
Element	T-41	T-38	T-44	T-51	T-82	T-25	T-2	175A	175B	213
SiO_2 (%)	68.10	70.57	72.72	74.44	74.29	75.18	75.54	76.52	76.88	76.74
TiO_2	0.46	0.39	0.11	0.10	0.07	0.07	0.12	0.05	0.03	0.04
Al_2O_3	16.52	14.78	14.67	14.07	14.04	13.68	13.32	12.79	12.79	13.02
Fe_2O_3	0.64	0.40	0.56	0.40	0.24	0.16	0.32	1.27	1.28	1.07
FeO	2.95	2.30	1.35	1.14	0.93	0.93	0.86			
MnO	0.06	0.09	0.07	0.05	0.05	0.04	0.04	0.03	0.03	0.03
MgO	0.96	0.77	0.21	0.24	0.11	0.08	0.14	0.03	0.03	0.05
CaO	3.05	2.60	1.20	1.24	1.11	0.95	0.87	0.66	0.64	0.67
Na_2O	3.55	3.18	3.76	3.60	3.66	3.50	3.43	3.54	4.15	3.60
K_2O	3.05	3.57	4.63	4.28	4.77	4.85	4.31	4.88	4.11	4.84
P_2O_5	0.14	0.11	0.06	0.06	0.05	0.02	0.05	<0.01	<0.01	<0.01
H_2O^+	0.54	0.70	0.63	0.21	0.38	0.50	0.31			
H_2O^-	0.22	0.20	0.26	0.38	0.28	0.14	0.32			
ILO								0.42	0.42	0.54
Total	100.24	99.66	100.23	100.21	99.98	100.10	99.63	100.19	100.36	100.60
V (ppm)	51	44	5	6	3	4	8	3	1	<1
Cr	20	40	23	<4	<4	36	37	<4	<4	<4
Ni	8	6	10	7	5	13	14	8	14	7
Zn	105	56	73	31	27	20	31	20	25	23
Ga	22	19	21	19	21	21	18	21	26	20
Rb	152	168	263	228	275	324	289	372	397	389
Sr	342	259	108	83	64	48	41	16	2	14
Y	24	24	42	56	54	74	85	82	206	76
Zr	241	163	181	107	80	77	99	96	196	80
Nb	9	8	13	11	10	14	17	15	38	14
Sn	4.4	4.1	10.5	3.4	2.4	2.1	5.1	2.6	4.5	4.3
Cs	5.0	4.9	13	6.3	5.7	5.1	8.6	8.6	9.4	11
Ba	1206	704	757	259	215	178	112	60	2	29
La	53	30	36	24	21	19	19	19	9	19
Ce	101	60	72	51	47	40	37	44	22	43
Pr	10.8	7.0	8.5	6.1	6.0	5.3	4.7	6.5	3.6	6.4
Nd	39	26	30	22	22	20	18	24	17	25
Sm	6.0	4.5	5.6	5.2	5.8	6.0	5.6	7.6	7.9	7.7
Eu	1.43	0.96	0.97	0.45	0.43	0.25	0.36	0.09	0.01	0.14
Gd	5.4	4.0	5.1	5.1	5.1	4.8	5.1	6.2	8.6	6.3
Tb	0.7	0.6	1.0	1.2	1.1	1.4	1.4	1.6	2.7	1.8
Dy	3.6	3.7	5.5	7.7	7.4	8.6	10.5	11.1	20.5	12.3
Ho	0.6	0.6	1.1	1.4	1.4	1.7	2.0	2.0	4.0	2.1
Er	2.2	2.2	4.2	5.5	5.2	6.1	8.2	6.6	15.3	5.7
Tm	0.4	0.4	0.8	1.1	0.7	1.0	1.4	1.2	2.8	1.2
Yb	2.3	2.4	4.6	5.9	5.7	8.6	11.5	8.5	20.4	8.0
Lu	0.3	0.4	0.7	0.9	0.7	1.1	1.6	1.2	3.2	1.0
Hf	5.5	4.3	4.7	3.5	2.7	3.2	4.0	3.8	9.1	3.7
Ta	0.7	0.7	1.6	1.5	0.9	1.7	2.0	1.4	2.1	1.8
Pb	14	20	46	28	31	30	36	30	40	31
Th	17	17	25	25	27	24	26	40	74	33
U	4.1	4.0	3.2	3.3	5.2	7.0	10.3	17.1	10.6	13.6
REE	253.18	168.89	216.84	196.01	183.88	190.52	208.70	217.50	313.70	208.54
Sm/Nd	0.15	0.18	0.19	0.23	0.27	0.30	0.31	0.31	0.47	0.31
Rb/Sr	0.41	0.61	2.22	2.53	3.73	6.00	6.02	18.88	84.50	20.87
Th/U	4.10	4.41	7.88	7.47	5.28	3.40	2.49	2.35	6.96	2.44
10000Ga/Al	2.49	2.40	2.72	2.49	2.77	2.83	2.55	3.11	3.79	2.97
Y/Nb	2.77	3.29	3.05	5.44	5.22	4.79	4.90	5.05	4.63	4.85
Nb/Ta	12.04	10.83	8.46	7.17	11.00	8.24	8.24	10.55	18.11	8.03
Zr/Hf	41.39	29.59	38.33	29.08	30.27	27.18	24.01	21.90	18.82	19.94
A/CNK	1.12	1.07	1.10	1.10	1.02	1.07	1.12	1.04	1.03	1.05
TFeO/MgO	3.68	3.46	8.85	6.27	10.44	13.44	8.22	34.99	0.69	19.07

Appendix 3 Continued.

	Naegi									
Element	211	70N505	70N506	70N508	70N509	70N510	T-139	T-97	T-105	T-110
SiO_2 (%)	77.38	76.74	77.15	76.64	76.02	76.20	65.53	68.06	70.03	72.10
TiO_2	0.05	0.03	0.04	0.11	0.05	0.05	0.55	0.52	0.29	0.24
Al_2O_3	12.67	12.65	12.40	12.49	12.61	12.69	16.60	14.96	14.83	14.36
Fe_2O_3	0.98	0.90	1.01	1.46	1.05	1.13	0.60	0.60	0.40	0.48
FeO							3.84	3.20	2.14	1.58
MnO	0.02	0.02	0.03	0.03	0.03	0.03	0.07	0.11	0.07	0.04
MgO	0.04	0.04	0.06	0.09	0.00	0.01	1.30	1.45	0.70	0.47
CaO	0.61	0.60	0.72	1.15	0.69	0.70	4.03	3.71	2.29	2.20
Na_2O	3.76	3.34	3.36	3.31	3.63	3.58	3.15	2.84	3.05	3.46
K_2O	4.54	5.07	4.72	4.25	4.78	4.85	2.78	3.10	5.10	3.82
P_2O_5	<0.01	<0.01	<0.01	0.01	<0.01	<0.01	0.13	0.12	0.09	0.07
H_2O^+							0.82	0.67	0.48	0.57
H_2O^-							0.32	0.38	0.36	0.32
ILO	0.76	0.54	0.38	0.44	0.40	0.41				
Total	100.81	99.93	99.87	99.98	99.26	99.65	99.72	99.72	99.83	99.71
V (ppm)	1	<1	<1	4	2	<1	22	36	27	10
Cr	<4	<4	<4	<4	<4	<4	<4	7	<4	<4
Ni	9	11	6	4	8	8	6	5	6	2
Zn	22	23	20	21	19	19	45	53	47	42
Ga	19	20	19	18	20	20	18	17	18	20
Rb	394	375	307	221	331	326	166	136	221	161
Sr	6	12	22	70	13	17	150	212	185	186
Y	95	127	68	52	100	93	43	35	36	35
Zr	77	96	108	98	92	86	135	145	148	133
Nb	12	17	12	12	13	16	7	7	8	8
Sn	3.7	3.3	2.6	1.7	2.7	1.1	2.7	3.2	2.8	1.9
Cs	12	7.2	9.1	4.4	9.4	5.3	5.5	4.9	4.0	4.1
Ba	8	40	60	331	29	58	219	426	937	617
La	16	22	23	34	26	23	25	28	19	39
Ce	44	48	54	72	55	56	44	56	41	78
Pr	7.0	7.4	6.9	8.7	8.3	7.1	6.2	6.9	5.0	9.3
Nd	28	30	28	33	33	29	22	24	19	32
Sm	9.2	9.8	6.9	7.3	9.8	7.3	4.8	4.7	3.7	6.8
Eu	0.05	0.08	0.20	0.36	0.07	0.11	0.68	0.96	1.03	0.86
Gd	8.4	9.0	6.3	5.5	8.2	7.1	4.0	4.2	3.8	4.7
Tb	2.4	2.4	1.6	1.3	2.4	1.9	0.9	0.9	0.9	1.0
Dy	15.9	16.9	10.1	8.5	14.6	12.5	5.9	5.4	5.5	4.9
Ho	2.6	3.5	1.8	1.4	2.7	2.4	1.2	0.9	1.0	0.9
Er	8.2	9.8	6.0	4.8	8.9	8.4	3.4	2.9	3.2	3.3
Tm	1.4	2.0	1.1	0.9	1.6	1.4	0.7	0.6	0.5	0.4
Yb	8.9	12.0	7.8	5.6	10.4	9.5	5.1	5.0	4.7	2.8
Lu	1.2	1.6	1.0	0.7	1.3	1.1	0.6	0.6	0.6	0.4
Hf	3.1	4.3	4.3	3.7	4.6	3.9	3.8	4.7	4.1	3.6
Ta	1.5	2.0	1.4	1.2	1.6	1.8	0.9	1.1	1.2	0.7
Pb	32	32	27	21	28	29	21	22	29	21
Th	44	22	33	21	32	31	16	15	13	16
U	7.0	10.1	6.4	4.7	6.4	7.3	5.4	4.2	3.3	1.8
REE	237.48	285.28	214.11	231.35	275.02	254.02	165.54	176.59	145.22	215.88
Sm/Nd	0.33	0.33	0.24	0.22	0.30	0.25	0.22	0.20	0.2	0.21
Rb/Sr	40.50	24.68	11.48	2.73	19.20	15.16	1.03	0.63	1.11	0.80
Th/U	6.29	2.23	5.11	4.49	5.08	4.25	2.95	3.70	3.82	9.14
10000Ga/Al	2.82	2.98	2.87	2.78	3.00	3.02	2.07	2.14	2.23	2.69
Y/Nb	7.05	6.47	4.95	4.01	6.99	5.56	5.70	4.86	4.48	3.79
Nb/Ta	7.80	8.44	8.82	9.47	8.39	8.90	8.05	6.98	6.9	11.70
Zr/Hf	26.63	18.56	21.61	27.83	19.00	22.04	34.00	26.45	28.6	30.68
A/CNK	1.04	1.05	1.04	1.03	1.02	1.02	1.03	1.00	0.97	1.04
TFeO/MgO	22.27	23.38	15.56	15.43	none	102.70	3.37	2.58	3.58	4.29

Appendix 3 Continued.

	Ryoke Belt					
Element	T-109	T-114	T-94	T-60	T-145	T-70
SiO_2 (%)	73.04	72.67	73.42	76.17	74.54	74.96
TiO_2	0.15	0.14	0.26	0.10	0.14	0.12
Al_2O_3	15.28	14.94	13.66	13.06	14.06	13.92
Fe_2O_3	0.32	0.40	0.60	0.16	0.28	0.36
FeO	1.15	1.15	1.62	0.86	1.04	0.83
MnO	0.06	0.04	0.07	0.02	0.08	0.07
MgO	0.26	0.19	0.51	0.06	0.29	0.27
CaO	1.93	1.82	1.53	1.09	1.12	1.22
Na_2O	3.01	3.05	3.14	3.29	3.29	2.93
K_2O	4.02	4.35	4.22	4.49	4.16	4.50
P_2O_5	0.04	0.03	0.09	0.02	0.04	0.03
H_2O^+	0.27	0.57	0.52	0.32	0.45	0.38
H_2O^-	0.26	0.42	0.16	0.20	0.34	0.24
ILO						
Total	99.79	99.77	99.80	99.84	99.83	99.83
V (ppm)	4	3	11	2	6	3
Cr	<4	<4	<4	<4	<4	14
Ni	4	2	5	9	4	7
Zn	20	27	38	29	32	33
Ga	15	15	16	20	16	16
Rb	195	136	209	240	263	294
Sr	76	147	137	49	68	53
Y	30	18	44	57	33	67
Zr	63	72	132	91	68	64
Nb	5	5	11	11	6	8
Sn	1.3	1.0	4.1	1.6	5.5	4.2
Cs	2.7	2.6	5.2	4.1	9.9	7.4
Ba	416	812	453	253	232	93
La	12	36	32	31	15	26
Ce	31	60	62	70	31	31
Pr	3.0	8.7	7.5	9.1	3.8	7.7
Nd	10	31	25	32	13	29
Sm	2.6	4.8	5.4	8.0	2.7	7.7
Eu	0.47	0.88	0.65	0.43	0.36	0.36
Gd	2.3	4.1	4.1	6.1	2.9	5.7
Tb	0.6	0.7	1.0	1.5	0.7	1.6
Dy	3.4	2.9	5.5	7.9	3.8	8.9
Ho	0.8	0.5	1.2	1.6	0.7	1.8
Er	3.0	1.2	4.2	5.0	2.8	6.6
Tm	0.6	0.2	0.7	0.8	0.4	1.1
Yb	3.4	1.3	5.8	4.6	3.4	7.4
Lu	0.4	0.2	0.7	0.6	0.6	1.1
Hf	2.3	2.1	4.4	3.0	2.7	2.6
Ta	1.0	0.3	1.1	1.0	1.1	1.6
Pb	30	19	30	29	31	44
Th	25	14	23	23	18	23
U	4.4	1.9	3.6	3.5	6.9	6.9
REE	102.02	168.32	198.11	231.59	110.76	196.10
Sm/Nd	0.25	0.15	0.22	0.25	0.20	0.27
Rb/Sr	2.34	0.82	1.37	4.44	3.33	5.04
Th/U	5.71	7.24	6.34	6.54	2.63	3.41
10000Ga/Al	1.83	1.92	2.26	2.82	2.19	2.18
Y/Nb	5.87	3.38	3.80	4.68	4.88	7.36
Nb/Ta	4.71	13.55	10.28	11.90	5.64	5.16
Zr/Hf	28.66	40.27	27.28	34.64	25.20	20.52
A/CNK	1.21	1.16	1.09	1.06	1.14	1.10
TFeO/MgO	5.54	7.97	4.25	16.76	4.46	4.29

日本の中部地方の対照的に異る化学的性質を持つ白亜紀後期ー古第三紀花崗岩類の成因

石原舜三・呉澄宇

要　旨

白亜紀後期－古第三紀の流紋岩類（11試料）と花崗岩類（白川29，土岐7，苗木9，領家10，合計55試料）について，XRF と ICP-MS 法により11主成分，32微量成分について分析した．白川地域の花崗岩類は飛騨変成帯に貫入し，Ｉタイプ磁鉄鉱系に属する花崗岩－花崗閃緑岩からなり，鳩ケ谷岩体北部では苦鉄質アンクラーヴが優白質花崗岩に混在する．白川花崗岩類はハーカー図上で高ナトリウム組（モンゾ閃緑岩－花崗閃緑岩）と低ナトリウム組（花崗岩）とに分けられる．前者は同様な化学的特徴を持つ，現在の飛騨帯に見られるような苦鉄質火成岩起源の変成岩類や花崗岩類に由来するものと考えられる．一方，花崗岩はハプロ花崗岩と呼べる珪長質度を持ち，その Rb/Sr 比は分別残液に見られる高い値を示さず，これは中性火成岩の部分溶融に由来するマグマの初期溶融相と判断される．共に Y，HREE に乏しく，源物質に柘榴石などの存在が推察される．

山陽－領家帯の白亜紀後期－古第三紀の花崗岩類は美濃帯とその南方延長部の領家変成岩類に貫入するＩタイプチタン鉄鉱系であり，山陽帯の土岐・苗木花崗岩では浅部相，南部の領家花崗岩ではやや深部相が産出している．これらはパーアルミナスかつチタン鉄鉱系である点で，起源物質として Al，C に富む堆積岩類との関連，更に角閃石含有相には火成岩起源が想定される．土岐・苗木花崗岩は親石元素に富むが，苗木花崗岩では特に Rb，Y，Th，U および Rb/Sr が高い．その REE パターンは HREE に富むフラット型で著しい負の Eu 異常を示し，これが分化したＩタイプマグマから固結したことを暗示する．